Ph.D. Thesis

Immunohistochemical investigations of the neuronal changes induced by chronic recurrent seizures in a pilocarpine rodent model of temporal lobe epilepsy

Norbert Károly M.Sc.

Experimental and Clinical Neuroscience Doctoral Programme
Doctoral School of Theoretical Medicine

Supervisors: Endre Dobó M.Sc., Ph.D.; András Mihály, M.D., PhD., D.Sc.

Department of Anatomy, Histology and Embryology
Faculty of Medicine
University of Szeged

Szeged
2017

LIST OF PUBLICATIONS RELATED TO THE THESIS

I. **Karoly N**, Mihaly A, Dobo E (2011) Comparative immunohistochemistry of synaptic markers in the rodent hippocampus in pilocarpine epilepsy. Acta Histochem 113:656-662.

II. **Karoly N**, Dobo E, Mihaly A (2015) Comparative immunohistochemical study of the effects of pilocarpine on the mossy cells, mossy fibres and inhibitory neurones in murine dentate gyrus. Acta Neurobiol Exp 75(2):220-237.

III. Dobo E, Torok I, Mihaly A, **Karoly N**, Krisztin-Peva B (2015) Interstrain differences of ionotropic glutamate receptor subunits in the hippocampus and induction of hippocampal sclerosis with pilocarpine in mice. J Chem Neuroanat 64-65:1-11.

Abbreviations

CGRP: calcitonin gene-related peptide

CR: calretinin

DAB: diaminobenzidine

DG: dentate gyrus

DSHS: densely-spiny hippocampal cells projecting to the medial septum

GC: granule cell

GAP-43: growth-associated phosphoprotein

GluA: AMPA ionotropic glutamate receptor

GluK: kainate ionotropic glutamate receptor

GluN: NMDA ionotropic glutamate receptor

iGluR: ionotropic glutamate receptor

IML: internal molecular layer

IR: immunoreactive

MC: mossy cell

MF: mossy fibre

MFS: mossy fibre sprouting

MSDB: medial septum-diagonal band of Broca complex

NeuN: neuronal nuclear protein

NPY: neuropeptide-Y

PB: phosphate buffer

PC: pyramidal cell

PILO: pilocarpine

SE: status epilepticus

SGL: supragranular layer

SL: stratum lucidum

SLM: stratum lacunosum-moleculare

SR: stratum radiatum

SRS: spontaneous recurrent seizures

Syn-I: synapsin-I

TLE: temporal lobe epilepsy

1. INTRODUCTION

Animal epilepsy is characterized by spontaneous recurrent seizures (SRS). The seizures are involuntary motor episodes that can vary from brief and nearly undetectable muscle twitches to long periods of vigorous shaking. The animal seizures cause cell damage in the brain, which include characteristic neuronal death, synaptic plasticity and astrocytic swelling, similar to that observed in brain hypoxia (Meldrum 2002). Certain pharmacologically evoked animal convulsions induce significant neuronal degeneration in some limbic areas, such as the amygdala and hippocampus (Mello and Covolan 1996; Schauwecker 2012; Silva and Mello 2000). These hippocampal lesions resemble the neuropathological hallmarks of the human mesial temporal sclerosis, which is also referred to as hippocampal sclerosis (Falconer 1974).

Although, the hippocampus is pointed to as the most likely origin of chronic seizures, there has been much debate about whether the damaged hippocampus is the cause or the consequence of chronic seizures. Parallel studies in patients and animal models of this disorder indicate that the appearance of hypersynchronous neuronal discharges responsible for generating spontaneous behavioural seizures result from the loss of balance between the excitatory and inhibitory neuronal populations of the hippocampus.

Some neuropathological features of human TLE can be produced in rodents by a single injection of pilocarpine (PILO), a muscarinic agonist (Ben-Ari 1985, Nadler et al. 1980, Turski et al. 1984). This treatment induces status epilepticus (SE) in the animals within half an hour. Animals surviving SE may display SRS after a latent period, which lasts for weeks. Histological analyses of the treated animals revealed that PILO-induced SRS have severe impact on the hippocampus; variable degrees of loss of the pyramidal cells (PCs) and mossy cells (MCs) were found, while granule cells (GCs) seemed to be resistant, and reacted with intense mossy fibre sprouting (MFS) to the seizures (Dobó et al. 2015, Mello et al. 1993, Turski et al. 1983).

One of the principal cell types of the dentate gyrus (DG) is the GC. The perikarya of the GCs form a tightly packed thick layer. This cell has a typical cone-shaped spiny apical dendritic tree which extend throughout the molecular layer. The GCs give rise to unmyelinated axons, which Ramón y Cajal (1911) called mossy fibers (MFs), forming *en*

passant, glutamatergic synapses with the MCs, GABAergic interneurones and the PCs in the CA3 area. Those epileptic animals which exhibit SRS after the latency period are supposed to show intense and ectopic MFS into the supragranular layer (SGL) of the molecular layer (Longo et al. 2003, Marksteiner et al. 1990). This process is well detectable with the Timm's silver-sulphide method showing the zinc content of the synaptic vesicles (Haug 1967).

The pyramidal cell layer in the CA areas of the hippocampus is filled with densely packed, more or less triangular shaped PCs. These principal, glutamatergic cells of CA3 send their axon collaterals (the Schaffer collaterals) to CA1, while the PCs of CA1 have projections to the subiculum and the deep layers of the entorhinal cortex. The hippocampal PCs are vulnerable to the epileptic insult (Wasterlain et al. 1993). The loss of these cells occurs frequently in the CA1 area: this is a characteristic neuropathological symptom in the epileptogenesis. Evaluation of the degree of damage to the PCs is often made by the immunohistochemical detection of the neuronal nuclear protein (NeuN) antigene, which labels most of the hippocampal neurones (Korzhevskii and Gilyarov 2010).

The MC is the third type of the glutamatergic principal cells in the hilar area of the hippocampus. Their cell bodies are relatively large, often triangular or multipolar in shape. Their dendritic trees remain within the polymorphic layer (hilum). The axons develop plexuses within the hilum, innervating the GCs and GABAergic interneurones (Scharfman 1995) both ipsilaterally and contralaterally. A very dense axonal arborization from the MCs is found in the internal molecular layer (IML) of the DG (Laurberg and Sorensen, 1981; Frotscher et al. 1991; Buckmaster et al. 1992, 1996). There are well-documented immunhistochemical markers for the MCs, which are different is mice and rats. In mice, calretinin (CR) and GluA2 receptor subunit, whereas in rats, calcitonin gene-related peptide (CGRP) have been reported to be reliable immunhistochemical markers (Liu et al. 1996; Freund et al. 1997). The GluA2 can be detected in the perikarya of the MCs, whereas their axon terminals do not display immunoreactivity for this subunit. The other two markers are not restricted to the cell bodies, they are present in the axon terminals in the IML, as well. If these proteins have specific synapse-related functions, any change in the density of these synaptic markers in the IML may reflect the activities of the MCs.

Numerous types of interneurones have been identified in the hippocampus. A detailed overview of the characteristics of the various hippocampal interneurones has been published

by Freund and Buzsaki (1996). Many of these neurones can be identified on the basis of the preferred synaptic targets of their axons; there are interneurones, axons of which tend to terminate on dendrites, perikarya or axon hillocks, respectively. Interneurones have also been classified on the basis of their inputs, shape, electrophysiological and immunohistochemical features (for review see Freund and Buzsaki 1996). Most of these cells are GABAergic, but they are often capable to release neuroactive peptides, as well. One of these neuromodulators is the neuropeptide-Y (NPY) (Colmers and Bahh 2003).

In rats four types of neurones have been found to express NPY (Deller and Leranth 1990): type 1: medium-size multipolar or fusiform hilar neurones (64% of the total NPY-IR neurones); type 2: pyramidal basket cells with apical dendrites, which project to the outer molecular layer (20%); type 3: large multipolar neurones deep in the hilum (9%); type 4: multipolar neurones restricted to the molecular layer (7%). No NPY immunoreactivity was observed in the GCs or in the pyramidal cells of the hippocampus in control rodents (Deller and Leranth 1990, Freund and Buzsáki 1996). The expression of NPY increases dramatically in the interneurones of the DG after seizures (Colmers et al. 1988, Marksteiner et al. 1990). The elevated level of NPY has become a useful immunohistochemical marker of epileptic activity in the DG (Scharfman and Grey 2006).

There are wide synaptic layers in the DG and in the CA zones, which contain a lot of neuronal connections. The major hippocampal input derives from the entorhinal cortex. In addition, multiple synaptic contacts are established among the intrinsic neurones as well. The neuronal cell loss due to epileptic activity inevitably induces synaptic reorganization, which includes vacation of postsynaptic sites and axonal sprouting. The density of the synapses can be revealed by visualization of marker proteins, which are known to be present in both the excitatory and inhibitory synapses. One of the general protein constituents of the active synapses is synapsin I (Syn-I), which is localized to the presynaptic parts. Immunohistochemistry for Syn-I can be readily applied to evaluate the gross changes in the synaptic densities during the axon terminal degeneration and the synaptic reorganization (Greengard et al. 1993, Baldelli et al. 2007, Kopniczky et al. 2005).

Those GCs which lose synaptic inputs in epileptic brains are supposed to release growth factors to trigger axonal sprouting and to regain lost synaptic contacts (Zimmer 1973, Okazaki et al. 1999). A widely used marker protein of the axonal growth is growth-associated

phosphoprotein (GAP-43), which is a protein kinase C substrate (Lovinger et al. 1986). Expression of GAP-43 during embryonic growth (Casoli et al. 1996) and its re-expression in adults during attempted axonal regeneration, such as MFS, are well known (Benowitz et al. 1990).

The MFs are the axons of the GCs, which possess particularly high zinc content. This feature can be utilized to reveal the MFs in sections by means of the histochemical Timm's silver-sulphide method for traces of zinc (Danscher et al, 2004). The detection of PILO-induced MFS is important, because the degree of its progress is often supposed to be proportional to the severity of the changes in the neuronal circuitry in the DG. The degree of the MFS can be estimated through the semiquantitative analysis of the density of the ectopical MFs in the innermost sublayer of the IML, which is referred to as SGL.

It is well known that the persistent and repetitive seizures in human TLE may lead to hilar cell death in the DG (Babb et al. 1984; Margerison and Corsellis 1966, Mathern et al. 1997). The MCs, which represent one type of the principal neurones, send axons to the IML in several mammals (Buckmaster et al. 1996). Damage to the MCs, as described in both human TLE (Babb et al. 1984) and animal models (Nadler et al. 1980, Sloviter 1987), results in vacated postsynaptic sites on the dendrites of the GCs in the IML.

A possible correlation between the MFS and the other neuronal changes in the PILO-treated animals has been suggested (Mello et al. 1993). Direct evidence for this correlation was not available, because the zinc-histochemistry and the classical immunohistochemical methods were not used on tissues from the same animal.

In our experiments, we applied the Timm's method, and we found important individual differences in the responses of the GCs to the PILO treatment. The differences also included the variations of the susceptibility to the convulsant and the various degrees of behavioural changes (SRS). We supposed that the individual differences may have been reflected by the amount of the zinc-containing ectopic MFs in the SGL. Therefore, we elaborated a novel methodological approach, which supports the application of zinc staining and immunohistochemistry on the same animal, and allows comparative studies of the MFS and changes in the neuronal markers in convulsing animals.

The SRS is accompanied by synaptic reorganization in the hippocampus. Thus, we checked whether GAP-43 has a role in the sprouting process of the MFS. We also

investigated the Syn-I immunoreactivity whether the overall density of the synapses was changed in the IML.

The extent of the effects of PILO treatment on the MCs, interneurones and GCs differs considerably. Although these cells are highly interconnected, their simultaneous changes have not been examined yet. We investigated the simultaneous changes of these cells in the same animals by means of histochemical and immunohistochemical methods. Our special aim was to test whether the loss of MCs and MFS are coupled processes in PILO-treated murines. We assumed a positive correlation between the damage to the MCs and MF sprouting in the animals two months after PILO-induced SE. In order to either confirm or disprove this assumption, we used the above mentioned methodological approach to visualize the MCs and the ectopic MFs in the same animals with immunohistochemistry and zinc-detection.

The dormant basket cell hypothesis (Sloviter 1991) is one of the plausible theories for the epileptogenesis in the rodent PILO model of TLE, which assumes the role of the hilar interneurones in this progression. Therefore, the effects of PILO-induced SE on the GABAergic cells were investigated by detection of their typical neuropeptide contents such as NPY and parvalbumin.

The hippocampal principal neurones are glutamatergic. The vast majority of the hippocampopetal fibres, which derives from the entorhinal cortex predominantly via the perforant and temporoammonic pathways is also glutamatergic (Scimemi et al. 2005). The discrepancies between the responses of the animals to convulsants may be based on the amount and/or the composition of the functional ionotropic glutamate receptors (iGluRs). Since previous studies failed to find explanation for strain differences at the hippocampal receptor level (Schauwecker 2003, Kurschner et al. 1998), in the present experiments, we performed a detailed layer-to-layer analysis in order to reveal the possible strain-dependent differences in the densities of the iGluRs.

In our work, we treated rats and three mouse strains with PILO systemically. The animals exhibiting intense convulsions for at least 30 min were sacrificed after a 2-6-month survival period for comparative studies by means of immunohistochemistry. We sought answers for the following questions:

(1) Are there important interspecies differences in the epileptogenic processes in the rodent PILO model?

(2) What are the major interstrain neuropathological differences in the mice, which may account for the different susceptibilities of the strains to the convulsants?
(3) How do the densities of the hippocampal iGluR subunits change in the epileptic mice?
(4) Which are the most beneficial histological methods to confirm the epileptogenesis in the individual animals?

2. MATERIALS AND METHODS

2.1. Animal treatment with PILO

Male Wistar rats (220-300 g), CFLP, Balb/c and NMRI mice (25-30 g) were kept in a temperature controlled room under standard light/dark cycle, with food and water *ad libitum*. All experimental procedures were conducted according to the EU Directive (2010/63/EU) and to the Hungarian Animal Act. Specific approval of care and use of animals was obtained in advance from the Faculty Ethical Committee on Animal Experiments (University of Szeged).

The animals were injected intraperitoneally with doses of PILO (Sigma-Aldrich Co., St. Louis, MO, USA) that were suitably adjusted for the species and strains so as to cause only two-thirds of the animals to exhibit SE in order to diminish the mortality. In preliminary experiments, doses of 380, 190, 180 and 195 mg/kg PILO were found to be appropriate for Wistar rats, CFLP, Balb/c and NMRI mice, respectively.

The PILO-injected animals displayed various levels of salivation and motor convulsions. With the aforementioned PILO doses, half of the animals that exhibited SE died on the day of treatment. Ninety minutes after SE onset, the animals were injected with 10 mg/kg diazepam (Seduxen, Richter Gedeon, Budapest, Hungary) intraperitoneally. The control animals received the same volume of physiological saline, the solvent of PILO. The animals that developed SE during the treatment were studied. These animals are referred to as PILO-treated animals.

2.2. Surgical procedure for fornix lesion

A fimbria-fornix lesion was produced in 8 mice anaesthetized intraperitoneally with sodium pentobarbital (65 mg/kg body weight; Sigma-Aldrich, St. Louis, MO, USA). The mice were mounted in a stereotaxic apparatus. An L-shaped wire knife (0.7 mm wide) was introduced

into the brain through a small hole in the skull, 0.25 mm laterally to the midline and 0.1 mm caudally to the bregma, down to 3.5 mm below the dura. The wire knife was rotated to a distance of 0.25 mm in both directions to produce a lesion of the fornix according to the Mouse Brain atlas of Franklin and Paxinos (1997).

2.3. Tissue preparation

The PILO-treated and the control animals were sacrificed 2 months after the injections. The animals were deeply anaesthetized with diethyl ether and perfused through the ascending aorta with 0.3% sodium sulphide in 0.1 M phosphate buffer (PB), and then with 4% formaldehyde in PB. The brains were dissected and cryoprotected overnight in 30% sucrose in PB at 4 ^{o}C. Coronal plane brain sections were cut on a freezing microtome at a thickness of 24 µm on the subsequent days following fixation. The sections for immunohistochemistry were stored in PB containing 0.1% sodium azide in a refrigerator until processing, while the sections for the Timm's silver sulphide staining were mounted on glass slides (ChemMate Capillary Gap Plus Slides, DAKO A/S BioTek Solutions, USA), air-dried and stored in dark at ambient temperature until development.

2.4. Immunohistochemistry

The sections were treated with 0.5% Triton X-100 and 3% hydrogen peroxide in 0.1 M Tris-HCl; pH 7.6 (TB), and then with normal swine serum (1/10). The following primary antisera were used: rabbit anti-Syn-I (Chemicon, Temecula, CA, USA, 1/1000), sheep anti-NPY (Peninsula Laboratories, Belmont, CA, USA, 1/48000), goat anti-CR (Chemicon, Temecula, CA, USA, 1/2000), rabbit anti-CGRP (Sigma-Aldrich, St. Louis, MO, USA, 1/10000) and mouse anti-GAP-43 (Sigma-Aldrich, St. Louis, MO, USA, 1:1000), mouse anti-NeuN (Chemicon, Temecula, CA, USA, dilution: 1/8000), rabbit anti-GluA1 (Millipore, Temecula, CA, USA, 1/500), rabbit anti-GluA2 (Chemicon, dilution: 1/200), (Chemicon, dilution: 1/200), rabbit anti-GluA2/3 (Chemicon, dilution: 1/400); monoclonal rabbit anti-GluK2 (clone: EPR6307; Abcam, dilution: 1/3000); mouse anti-NMDAR1 (Abcam, dilution: 1/5000).

The sections were incubated under continuous agitation at room temperature overnight. After washing, the sections were incubated with the appropriate biotinylated secondary antibody (Jackson ImmunoResearch, West Grove, PA, USA, 1/500) for 90 min, and finally with peroxidase-labelled streptavidin (Jackson ImmunoResearch, West Grove, PA, USA, 1/1000) for 90 min. The sites of immunoreaction were visualized with 0.05% 3,3’-diaminobenzidine (DAB) and 0.01% hydrogen peroxide in TB.

2.5. Timm's silver sulphide method

The sections were processed for Timm's staining according to Danscher et al. (2004). The composition of the staining solution: 60 ml of 50% gum arabic, 10 ml of 2 M sodium citrate buffer (pH 3.7), 30 ml of 5.67% hydroquinone, and 0.5 ml of 17% silver nitrate solution. The sections were continuously agitated in a dark chamber for 50-60 min. It should be noted that in our preliminary studies 35 min development time revealed the zinc-containing elements in the hilum and SL appropriately, but the staining of the expected recurrent MFS in the IML required 50 min in rats and 60 min in mice. The staining process was terminated with 2% sodium acetate, and the unreacted silver ions were removed with 5% sodium thiosulphate. The sections were covered with DPX mounting medium.

2.6. Visualization of the fornix lesion

The correct site of the lesion was confirmed via the appearance of erythrocytes extravasated from the breached blood vessels, which exhibited peroxidase-like activity. The sections including the sites of lesions were treated by means of 0.05% DAB plus 0.01% hydrogen peroxide in TBS for 30 min. Thereafter, the sections were counterstained with haematoxylin for Nissl substance and cell nuclei.

2.7. Image analysis

Pictures were taken with an image-capturing system (Olympus DP50) attached to an Olympus BX-50 microscope (Soft Imaging System GmbH, Münster, Germany). Image analysis was performed with Adobe Photoshop 7 (Adobe Systems Incorporated, San Jose, CA, USA). The pixel density of the immunoreactivity was measured by a researcher blind to the experimental

conditions of the animals. Briefly: through use of the "marquee" tool, 8-12 circular selections of 0.1 mm diameter were made in immediately adjacent positions along the hippocampal layers. The average of 10 background determinations (carried out near the layers in neuropil sites without immunopositive staining) was subtracted from the average pixel densities measured within the hippocampal layers. Differences between the corresponding hippocampal regions of PILO-treated and control animals were assessed by using the unpaired one-tailed Student's *t* test. Data were analysed and plotted with the aid of GraphPad 4.0 (GraphPad Software, Inc, CA, USA). For every measurement, 8 hippocampal sections in the rat model and 12 sections in the mouse model were used from each animal. Pearson's correlation analyses were used to evaluate the relationship between the optical densities of NPY and Syn -I.

2.8. Cell count

The number of CR-IR hilar neurones were counted on 12 sections of each mouse DG, using Image-Pro Plus 4.5.1 (Media Cybernetics, Inc., USA) by a researcher blind to the experimental conditions. A cell was identified as one CR-IR neurone provided its at least 50 μm^2 exhibited an at least average pixel density of 60 above the background value. The total areas of DGs per mouse were summed, and the densities of CR-IR hilar neurones were determined as number per mm^2. The difference between the control and treated animals was evaluated by the unpaired one-tailed Student's *t* test.

3. RESULTS

3.1. Synaptic changes in the hippocampi of Wistar rats and CFLP mice

3.1.1. Mossy fibre sprouting

Our observations concerning the zinc-containing elements in the hippocampus are in good agreement with the literature findings (Cavalheiro et al. 1996, Lemos and Cavalheiro 1995). Timm's staining was localized in strongly stained varicose axons in the hilum and in the stratum lucidum (SL) (Fig. 1.). In the untreated animals, there was a weak homogeneous reaction in the IML in both rodent species (Fig. 1. A, C). In general, this staining was found to

be more constant and more intense in the rat than in the mouse. In mice, the staining density in the IML displayed considerable individual differences.

Mice. The animals, which exhibited SE, were checked for the presence of MFS. 41% (7/17) of the PILO-treated CFLP mice showed massive increases in the staining intensity of the hilum and the SL (Table 1.). The black infrapyramidal layer of region CA3, which contained Timm-positive MFs also increased in width. Moreover, dark zinc-containing varicose axons appeared within a narrow band adjacent to the GCs, *i.e.* in the SGL, which were interpreted as ectopic MFS (Fig. 1. D). Those animals which exhibited this ectopic MFS in the SGL were termed Timm-positive animals. The fornix lesion did not change the staining pattern or the intensity of the zinc histochemistry of the mouse hippocampus on either side after a survival period of 6-7 postoperative days.

Rats. 54% (7/13) of the PILO-treated rats displayed massive increases in the staining of the the hilum and the SL. In the Timm-positive rats, the zinc-positive elements disappeared from the outer zone of the IML, outside the SGL (Fig. 1. B). It should be noted that in the Timm-positive mice, despite the presence of ectopic MFS in the SGL, the staining did not vanish from the outer zone of the IML (compare Fig. 1. B and Fig. 1. D).

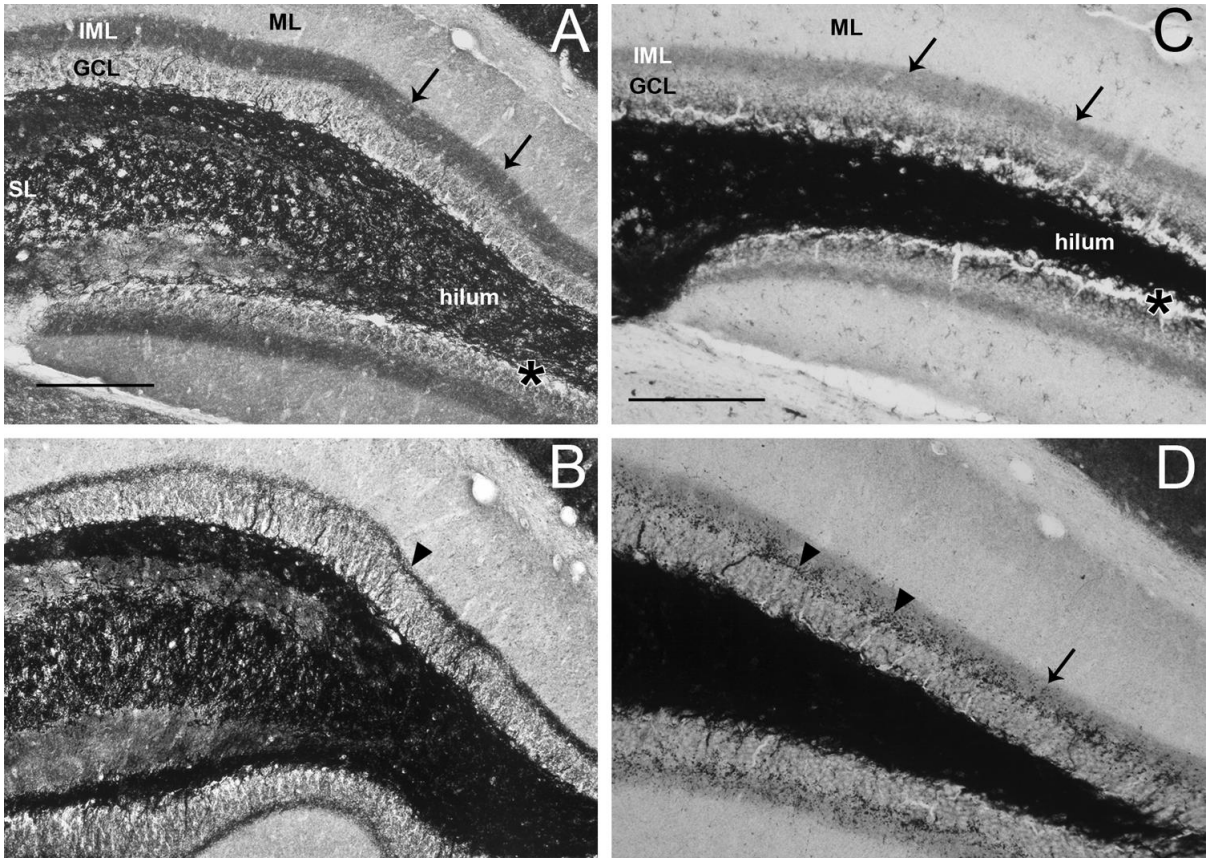

Fig. 1. Ectopic sprouting of MFs is induced by PILO treatment, as evidenced by Timm's staining. The hilum exhibits the highest density of zinc, and a distinct IML (arrows) is seen in the control animals (rat: A, mouse: C). In the PILO-responsive rats, the staining in the outer two-thirds of the IML has disappeared, while the zinc content remains in its inner one-third (*i.e.* the SGL) (arrowhead in B). In the PILO-responsive mice, the staining has not vanished in the IML (arrow in D), while the labelling in the SGL is enhanced (arrowhead in D). Artificial shrinkage is visible (asterisks in A and C). GCL: granular cell layer, IML: inner molecular layer, ML: molecular layer, SL: stratum lucidum. Scale bars: 100 µm (A and B), 150 µm (C and D).

3.1.2. Syn-I immunohistochemistry

Strong immunoreactivity for Syn-I was found in the MFs in both types of control rodents. The cell bodies were not labelled. The molecular layer was moderately positive (Fig. 2. A, C).

Mice. In the convulsing mouse, after 2 months survival, the density of immunostained elements in the SL was increased significantly in the Timm-positive animals as described by Károly et al. (2011 and 2015). Moreover, the layer displaying Syn-I immunostaining thickened considerably. The dentate hilum, which contains strongly-stained MF terminals, as verified by Timm's staining, displayed a highly significant drop in Syn-I staining intensity. In the IML, the overall staining did not change significantly (Fig. 2. C).

Rats. Analysis of the brain sections from PILO-treated and control rats revealed similarities and differences as compared with the mouse. The PILO-induced seizures enhanced the Syn-I immunoreactivity significantly in every layer (Fig. 2. B) in 69% (9/13) of the PILO-treated rats. In addition, Syn-I immunoreactivity appeared in the SGL of 46% (6/13) of the treated rats, which was absent in controls. This immunostaining displayed various intensity.

3.1.3. GAP-43 immunohistochemistry

In control animals, the hippocampal GAP-43 immunostaining was similar in the two rodent species. The most intense immunoreactivity was observed in the stratum lacunosum-moleculare (SLM) (Fig. 3.). Somewhat less, but strong and homogeneous staining was found in the IML of the dentate gyrus in both species. The hilum and the SL of CA3 field were devoid of staining. The principal neurones did not stain.

Mice. In the PILO-treated groups, the staining of the IML was reduced significantly (Fig. 3. C, D, Fig. 4. A). No differences were noted between the control and PILO-treated animals as to the GAP-43 staining in other hippocampal layers.

Rats. GAP-43 immunohistochemistry revealed significant reduction in the staining intensity of the IML (Fig. 3. A, B, Fig. 4. B). In contrast to the mouse, the IML of the rat was not a homogeneously stained band, rather it displayed a middle sublayer, where the GAP-43 immunoreactivity was reduced.

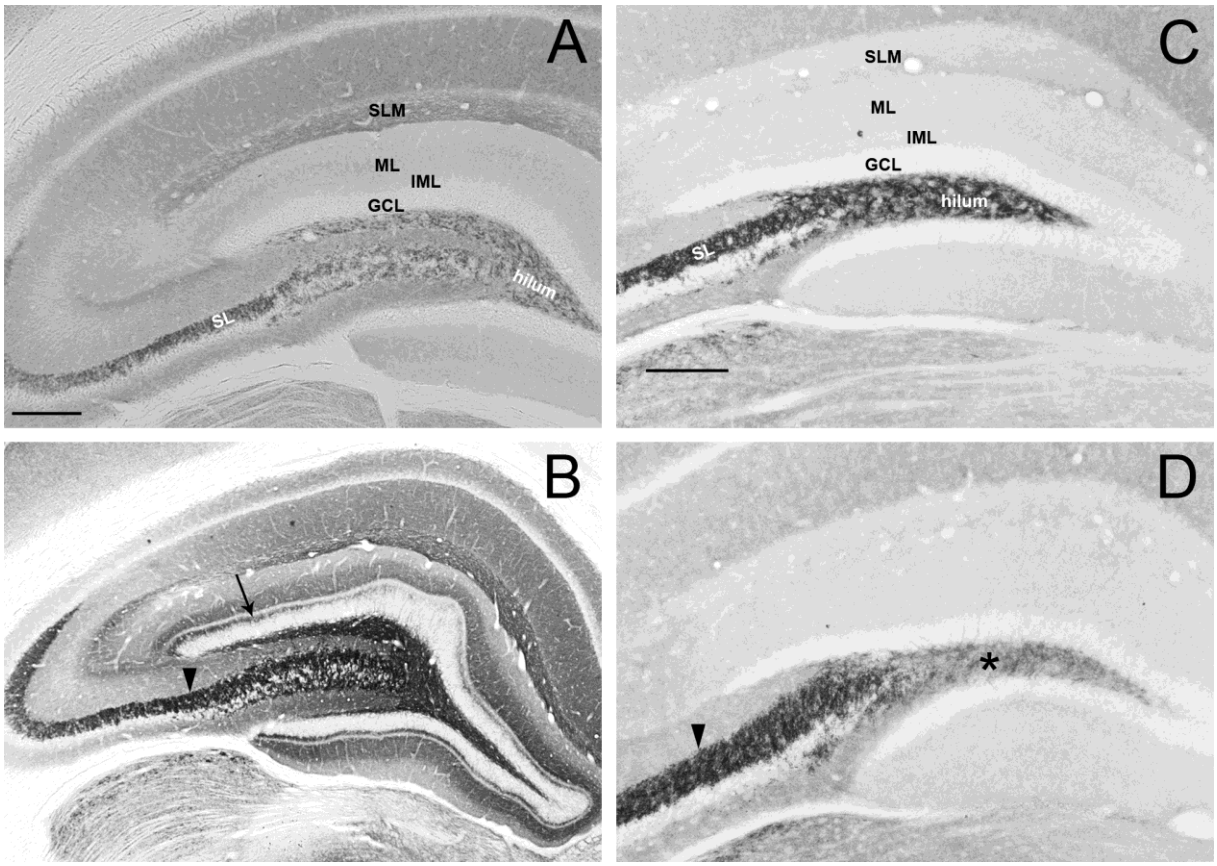

Fig. 2. Species-dependent changes in Syn-I immunoreactivity in the PILO-responsive rodents. Similar distributions of Syn-I are found in the control rat (A) and mouse (C) hippocampi.

In the rat, all the layers of the synaptic fields display increases to various extents in Syn-I immunoreactivity. The most characteristic increase is found in the SGL (arrow in B). In both the mouse and the rat, significantly enhanced immunoreactivity is seen in the SL (arrowheads), but a decrease is noted in the hilum of the PILO-responsive mouse (asterisks in D). GCL: granular cell layer, IML: inner molecular layer, ML: molecular layer, SL: stratum lucidum, SLM: stratum lacunosum-moleculare. Scale bars: 250 μm (A and B), 200 μm (C and D).

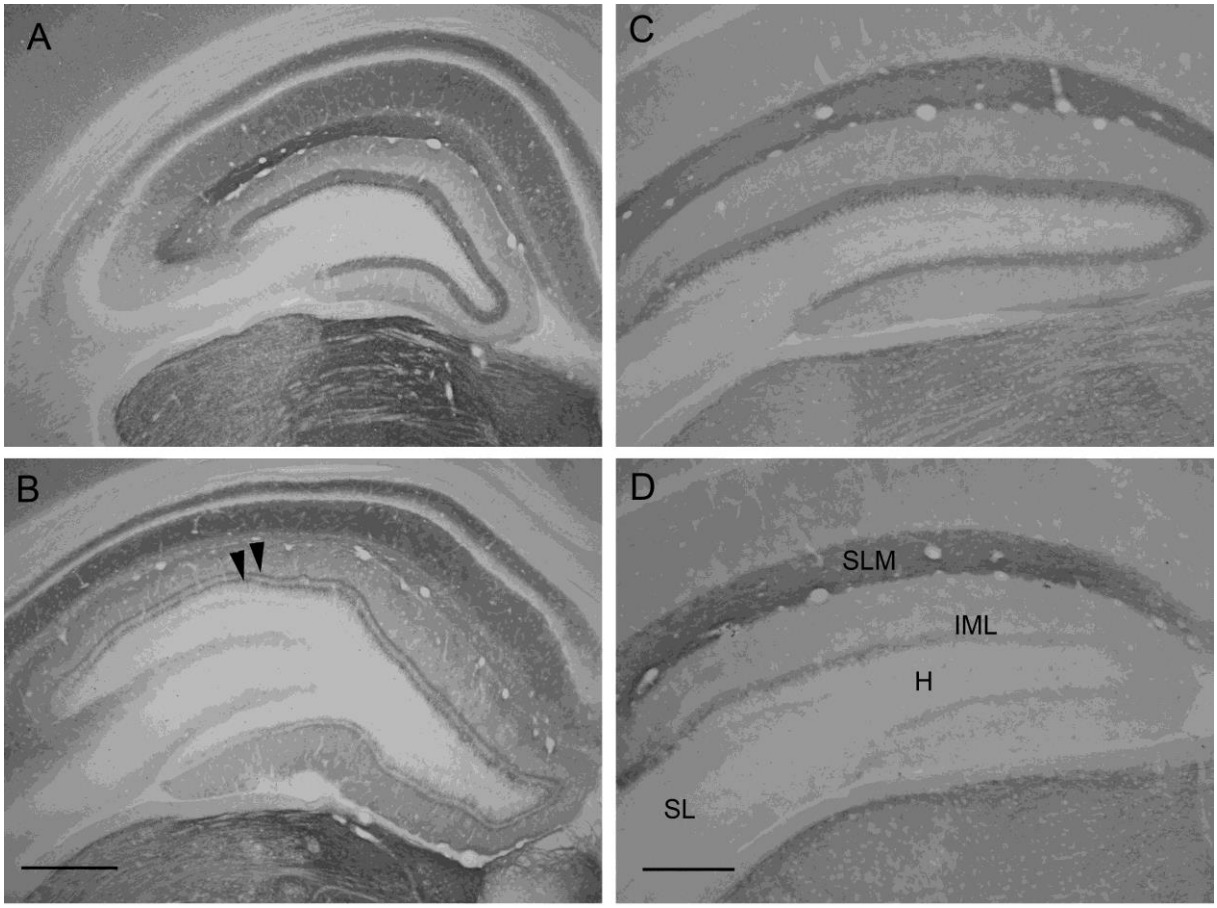

Fig. 3. (A) Control rat, (B) PILO rat, (C) control mouse and (D) PILO mouse. The GAP-43-positive band in the IML is thicker in the control animals while in the PILO-reacted rodents show paler bands furthermore the rat displays two thin bands (arrowheads). The most intense immunoreactivity was observed in the stratum lacunosum-moleculare. IML, internal molecular layer; SL, Stratum lucidum; H, hilum; SLM, stratum lacunosum-moleculare. Scale bars: 0.5mm (A and B); 200 µm (C and D).

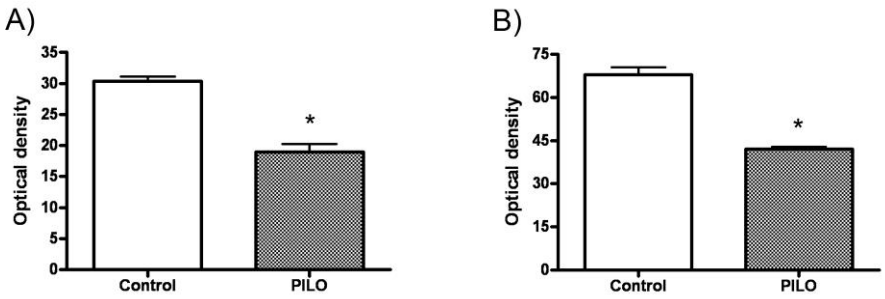

Fig. 4. Densitometry of GAP-43. GAP-43 immunoreactivity in the PILO-reacted mouse IML (A), GAP-43 immunoreactivity in the PILO-reacted rat IML (B). The density of the GAP-43-positive band was significantly higher for the controls than for PILO-treated animals among both rodents ($p < 0.0001$).

3.2. Interneuronal changes in the murine hippocampus

3.2.1. Effects of PILO on the NPY-immunoreactive interneurones

Moderate NPY immunostaining was found in small perikarya and their stem dendrites throughout the DG and the stratum oriens in the CA1 area of the control rats and mice, but not in the perikarya of the GCs or the pyramidal cells, as described earlier by Köhler et al. (1986). The staining patterns differed slightly between the two species (Fig. 5.). In the studied mouse strains (CFLP, Balb/c and NMRI), the staining of the neuropil within the layers of the DG was homogeneously and weakly punctuate (Fig. 5. C). The SLM displayed the highest immunoreactivity for NPY. In the rat, the strongest staining was observed in the molecular layer where the outer strip contained the highest density of NPY-IR dots (Fig. 5. A).

Mice. The effects of PILO-induced seizures on the distribution of NPY immunoreactivity were compared in three mouse strains. In the CFLP strain, the immunoreactivity was enhanced dramatically throughout the entire DG and the SL in 53% (9/17) of the PILO-treated animals (Table 1.). In Balb/c and NMRI strains, every animal displayed enhanced NPY staining. In the other parts of the hippocampus, including the SLM, no marked changes were observed in any of the strains. The immunoreactivity for NPY increased also in the molecular layer, but to a much lesser extent than in the areas of the MFs (Fig. 5. D). Characteristically, one band that seemed slightly narrower than the IML, *i.e.* the SGL, stood out from the homogeneously labelled plexiform layer in 41% (7/17) of the PILO-treated CFLP mice (Table 1.). The strong staining often concealed the NPY-IR neurones in the MF-containing areas. However, in other hippocampal areas the NPY-IR perikarya were not hidden by MFs, and they were immunolabelled much more intensely than those in the control mice. The intensity differences of the individual neurones were not quantified.

Hippocampal sclerosis was detected in some NMRI mice. In these hippocampi the lateral extent and the width of SL in the CA3a were dramatically reduced, but the NPY staining was strong. In these animals, the hilum of the DG was also strongly labelled, similarly to other PILO-responsive animals of the studied mouse strains. It is worth noting that in the other mouse strains we did not find sclerotic hippocampus.

Rats. The treatment with PILO resulted in similar changes in the rat hippocampus (Fig. 5. B). The NPY staining was attributed to nerve fibres and sharply demarcated the MF-containing hilum and SL in 69% (9/13) of the PILO-treated rats (Table 1.). The SGL was also revealed by NPY immunohistochemistry in 54% (7/13) of the PILO-treated rats (Table 1.).

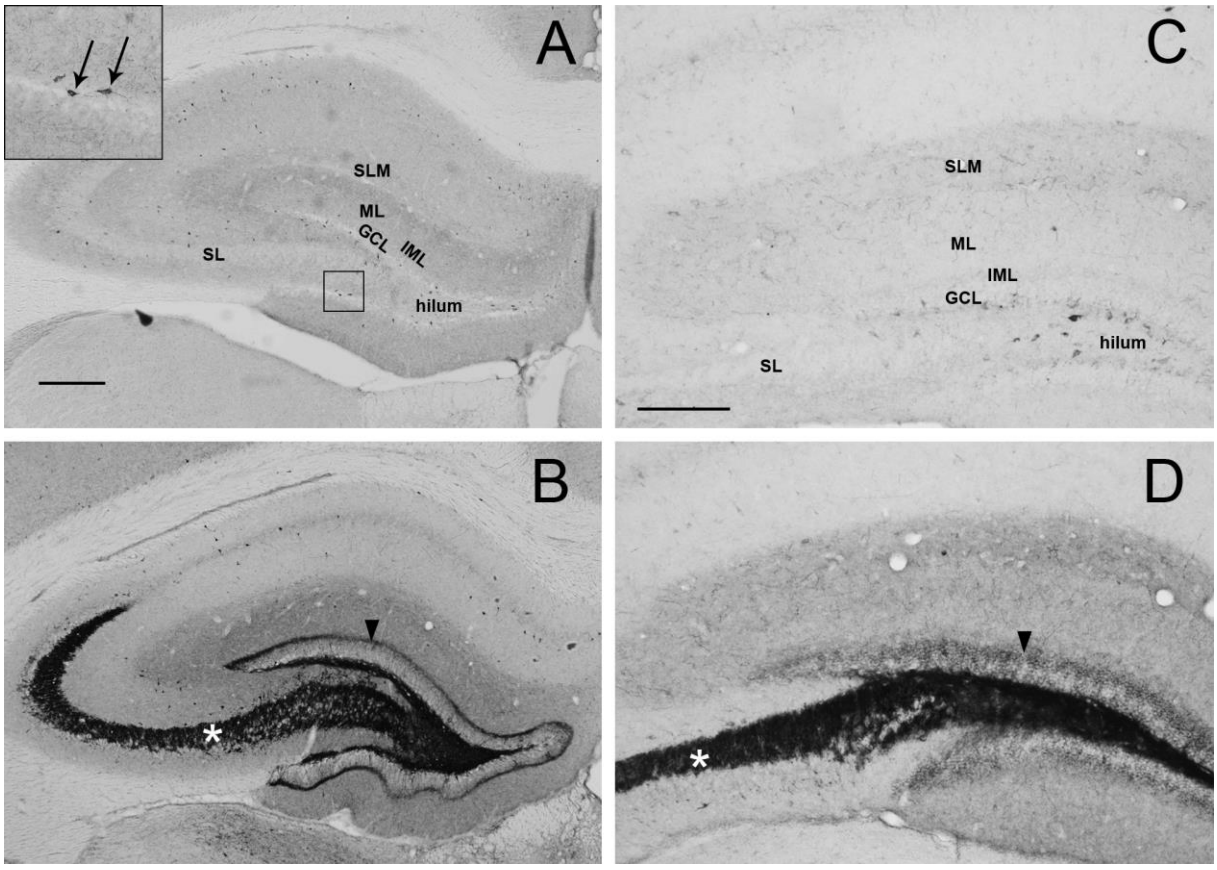

Fig. 5. PILO treatment increased the NPY immunoreactivity to a great extent in the rodent hippocampi. In the control sections (rat: A, mouse: C), the immunoreactivity is mainly confined to the cell bodies and larger processes (arrows in A inset). In the PILO-responsive animals (rat: B, mouse: D), the NPY immunoreactivity was dramatically increased in the SL (asterisks) and hilum, and moderately in the SGL (arrowhead). Scale bars: 250 μm (A and B), 200 μm (C and D).

3.2.2. Correlation analysis between NPY and Syn-I immunoreactivities

Since the PILO treatment altered the NPY and Syn-I immunoreactivities in the same layers in both species, and NPY and Syn-I were localized in axons, the possibility of a correlation between these elevated densities was probed in the affected areas in the individual animals. The data for semiquantitative analysis were collected from pairs of adjacent sections, the members of which were immunostained for NPY and Syn-I, respectively (Fig. 6.).

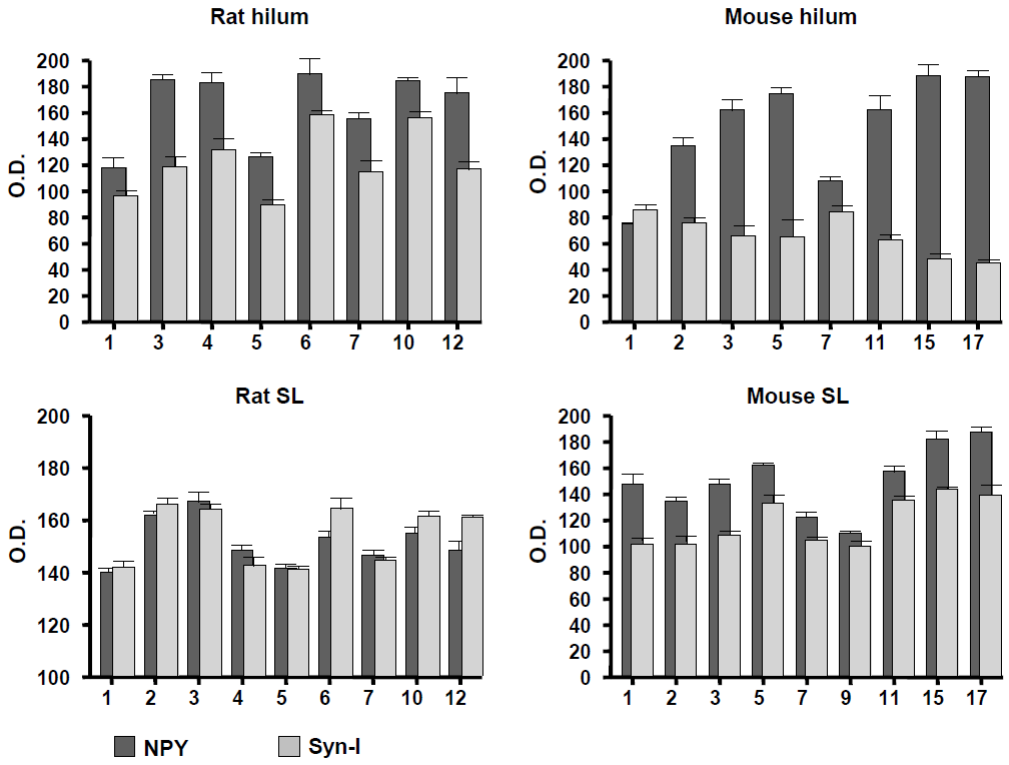

Fig. 6. Comparison of the changes in NPY and Syn-I immunoreactivities in the hilum and SL of the individual animals after PILO treatment. The numerals on the horizontal axes are the identification numbers of the animals used in the study (cf. the upper indices such as [2], [3] and [4] in Table 1). The optical density values (O.D.) were obtained by reduction of the values of the individual PILO-treated rodents from the average values of the controls. The PILO-treated individuals with unchanged immunoreactivity were not included in the graphs. The results of Pearson's correlation analyses are shown in Fig. 7.

Mice. Positive correlations were found between the two markers in the SL (R^2 Linear = 0.759) in the CFLP mouse. The increased density of the NPY immunoreactivity was inversely proportional to the density of Syn-I in the hilum (R^2 Linear = 0.832) (Fig. 7. C, D).

Rats. In the rat, positive proportional changes were found between the markers in the SL (R^2 Linear = 0.535) and in the hilum (R^2 Linear = 0.542) (Fig. 7. A, B).

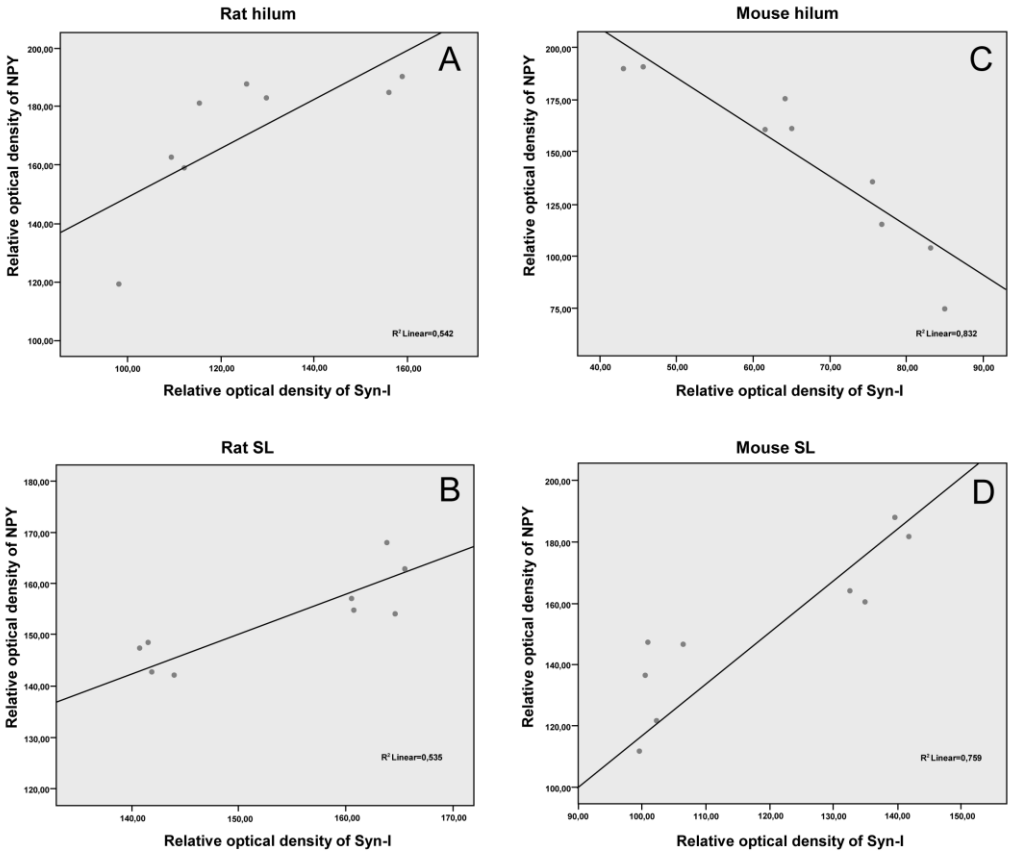

Fig. 7. Correlation analysis of the changes in NPY and Syn-I immunoreactivities induced by PILO treatment revealed a species difference between the rat and the mouse. The original data are shown in Fig. 6. The plotted data are derived from those PILO-responsive animals which displayed enhanced immunoreactivities in the hilum and SL, as indicated by the upper indices in Table 1. In the rat, positive proportional changes were found between the two markers in the hilum (R^2 Linear = 0.542) (A) and SL (R^2 Linear = 0.535) (B). However, in the mouse, the density of the immunoreactivity for NPY was inversely proportional to that for Syn-I in the hilum (R^2 Linear = 0.832) (C), while a positive correlation was also measured in the SL (R^2 Linear = 0.759) (D).

Although, frequent coincidence of NPY and Syn-I immunoreactivities in the SGL suggested a close relationship between these markers, our semiquantitative analysis did not show correlation in this narrow band (R^2 Linear = 0.023). However, the paired comparisons of the subsequent sections immunostained for NPY and Syn-I revealed that all the six animals which exhibited Syn-I immunoreactivity in the SGL were immunopositive for NPY, as well (Table 1.). It is worth noting that only four animals out of those six ones showing Syn-I immunoreactivity in SGL were found to exhibit Timm-positivity in this layer (Fig. 8.).

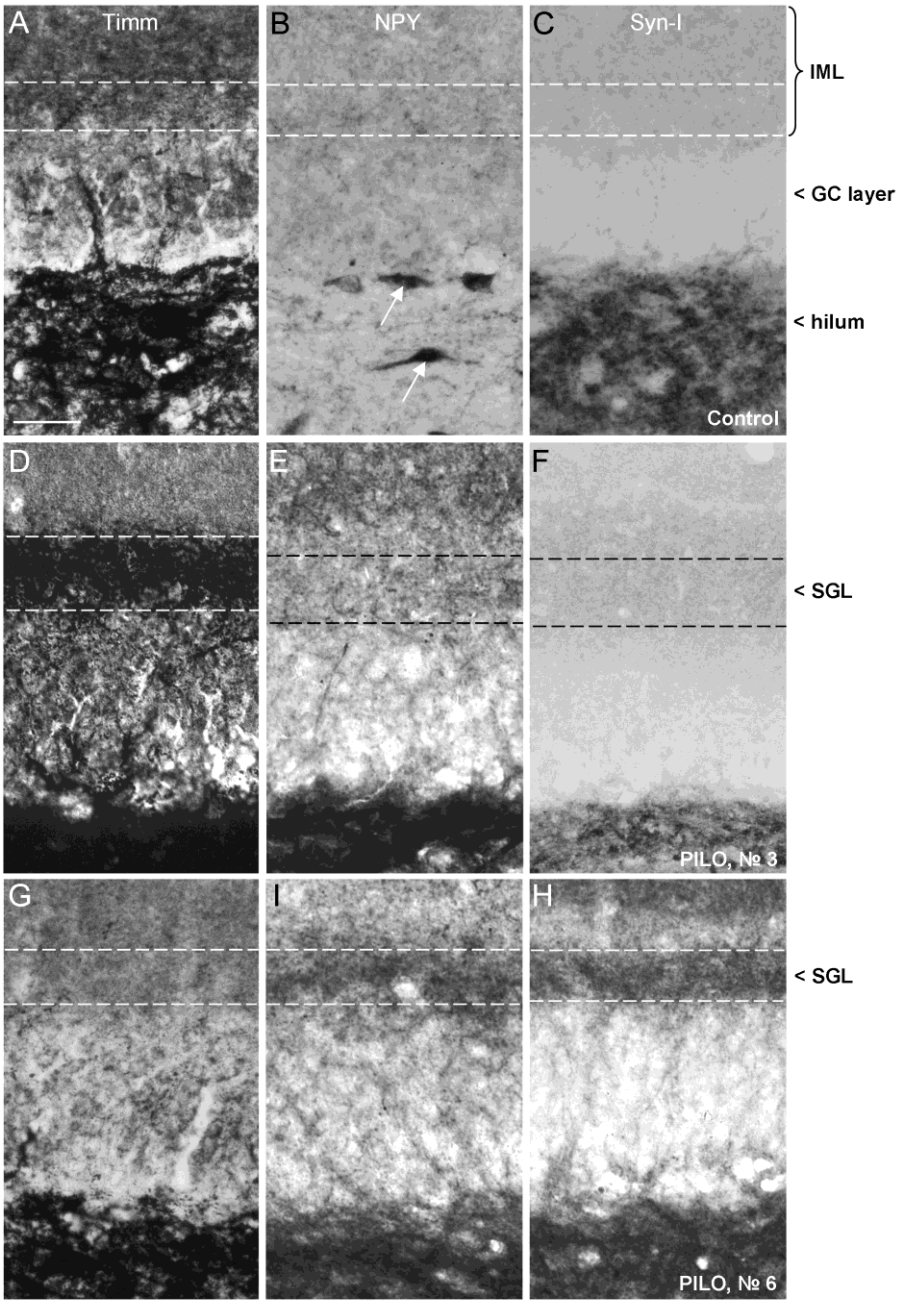

Fig. 8. Different ectopic fibres appeared in the SGL after PILO treatment. SGLs (outlined by dashed lines) of control (A-C) and PILO-treated rats #3 (D-F) and #6 (G-I) are compared after Timm's staining (A, D and G), and NPY (B, E and I) and Syn-I immunohistochemistry (C, F and H). PILO treatment resulted in "triple positive" SGL in 38% of the animals. Rat #3 displayed strong Timm-positive MF sprouting (D), but no NPY (E) and Syn-I (F) immunoreactivities in the SGL. In contrast, rat #6 showed no Timm staining (G), but intense NPY (H) and Syn-I-IR (I) puncta in the SGL. Some NPY-IR perikarya (arrows) stand out from the hilum in the control rat (B). The GCs remained unstained with the antibodies even in the intensely PILO-responsive animals (E-F, H-I). Scale bar: 50 µm.

3.3. Effects of seizures on principal neurones

3.3.1. Mouse mossy cells

Two immunohistochemical markers (CR and GluA2/3 subunit) have been used for the detection of the mouse MCs. The CR antibodies were applied to visualize the terminal fields of the axons in the CFLP mice. The CR immunoreactivity in the control mice was similar to that described by Liu et al. (1996). CR-IR somata and processes were seen in the DG, and a prominent IR band was observed in the IML.

The densities of CR-IR cells were compared in the control and PILO-treated CFLP strain (Fig. 9. A, B). Altogether 127 and 196 CR-IR cells were identified in the control and PILO-treated mice, respectively. In terms of density values (number per mm^2) no significant change was found. Representative sections were counterstained with cresyl violet for cell nuclei and Nissl substance. None of the counterstained sections showed noticeable cell loss in the DG in convulsing animals.

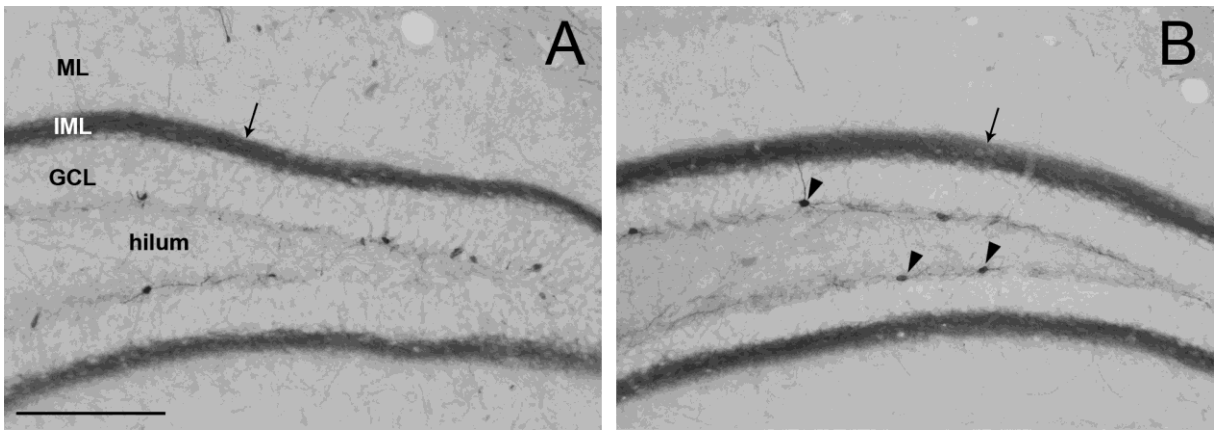

Fig. 9. No changes in CR immunoreactivity were induced by treatment with PILO in the mouse DG. Intense staining can be noted in the IMLs of both the control (A) and the PILO-responsive (B) mice (arrows). The CR-IR neurones survived the treatment (arrowheads). GCL: granular cell layer, IML: inner molecular layer, ML: molecular layer. Scale bar: 150 μm (A and B).

CR immunoreactivity in the IML did not change after PILO treatment (Fig. 9. A, B). Since some authors (Borhegyi and Leranth 1997, Maglóczky et al. 2000) have postulated that a considerable number of the CR-IR processes in the IML originate from the supramamillary nucleus through the fornix, this bundle of fibres was transected in 4 control animals, in order

to evaluate the proportions of the CR-IR synapses of the extra- and intrahippocampal sources. We found that fornix transection did not cause changes in the CR-IR pattern. Equally massive, homogeneous CR-IR bands were found in the IMLs on both sides. Similarly, no change was detected in the densities of the CR-IR cells in the hilum (Fig. 10.).

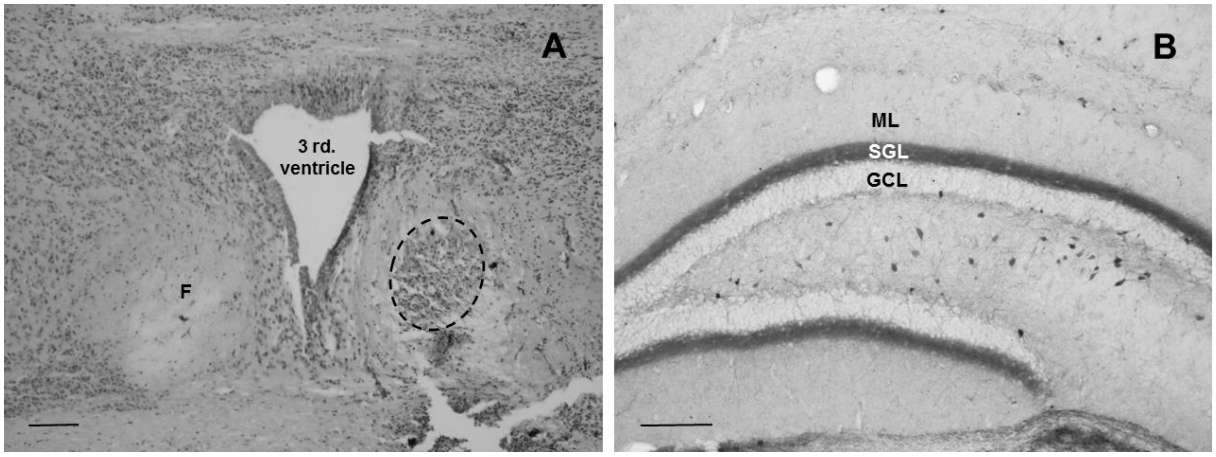

Fig. 10. The fornical lesion lacked effect on the CR-immunoreactive fibers in the IML. In the control mouse the fornix was transected unilaterally. The appearance of a pathological cell mass (enclosed by dashed line) confirmed the site of lesion as revealed by the Nissl staining (A). The density of the CR-immunoreactive fibers in the IML was not reduced (for comparison see Fig. 9) (B).
F: fornix, GCL: granular cell layer, IML: inner molecular layer, ML: molecular layer. Scale bars: 200 µm

The perikarya of the MCs were also verified by GluA2/3 antibodies in the Balb/c and NMRI mice. PILO-treatment resulted in significant changes in the immunoreactivity for this AMPA subunit in the hilum. The density of the MCs was reduced in both mouse strains significantly (-29% for Balb/c and -62% for NMRI) (see for details in Chapter 3.4.1.).

3.3.2. Rat mossy cells

Presence of CGRP in the rat hilar cells is an accepted marker for MCs (Freund et al. 1997). CGRP immunohistochemistry displayed the most intense staining in the IML in the control animals, in accordance with earlier observations. Moreover, various numbers of weakly stained CGRP-IR multipolar neurones were also scattered in the hilum (Fig. 11. A). Labelled neuronal elements were not found outside the DG.

The PILO treatment resulted in marked changes in the CGRP immunoreactivity. The CGRP-IR staining disappeared from the IML in 69% (9/13) of the PILO-treated rats (Table 1.). The number of the CGRP-IR hilar neurones was reduced to 4% of the control values ($p<0.05\%$) (Fig. 11. B).

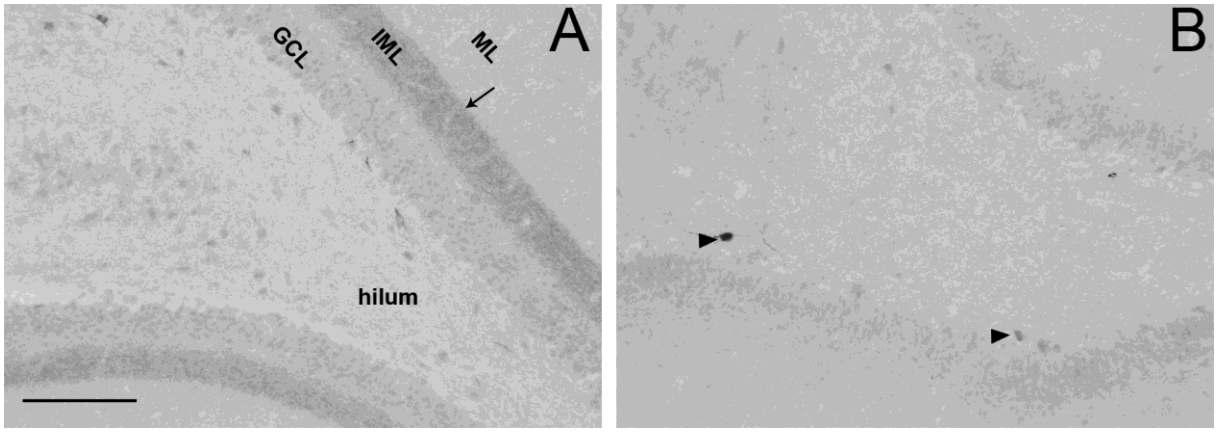

Fig. 11. Reduction in CGRP immunoreactivity in the PILO-responsive rats. In a control rat (A), the DG displays a prominent CGRP-IR IML (arrow), which vanished after PILO treatment (B). A few immunopositive hilar cells survived the treatment (arrowheads). GCL: granular cell layer, IML: inner molecular layer, ML: molecular layer. Scale bar: 100 μm (A and B).

3.3.3. Comparative analysis of the effects of PILO on the mossy cells, mossy fibres and interneurones

Mice. Whereas no changes were observed in the CR immunostaining of the mouse DG, marked enhancements were found in the density of MFs and NPY immunoreactivity (Table 1.). In summary, one-fifth more animals displayed alterations in the NPY immunoreactivity than in Timm's staining (53% vs. 41%). Among those individuals that showed any changes in either Timm's staining (7/17) or NPY immunostaining (9/17), 6 animals (6/17) displayed similar changes, *i.e.* double positivity for the ectopic appearance of zinc and NPY in the SGL. Two mice exhibited opposite changes in the SGL: one Timm-positive mouse was negative for a NPY-IR SGL (though the immunoreactivity was increased in the hilum and the SL) (see mouse № 7 in Table 1.) and one Timm-negative mouse (*i.e.* without ectopic MFS) was positive for a NPY-IR SGL (see mouse № 2 in Table 1.).

Mouse #	CR[1]	Timm[2]	NPY
1	ND	+ (weak)	+[2,3,4]
2	ND	-	+[2,3,4]
3	ND	+	+[2,3,4]
4	ND	-	-
5	ND	+	+[2,3,4]
6	ND	-	-
7	ND	+ (weak)	+[3,4]
8	ND	-	-
9	ND	-	+[3]
10	ND	-	-
11	ND	+	+[2,3,4]
12	ND	-	-
13	ND	-	-
14	ND	-	-
15	ND	+	+[2,3,4]
16	ND	-	-
17	ND	+	+[2,3,4]
		7/17 (41%)	9/17 (53%)

Rat #	CGRP[1]	Timm[2]	NPY	Syn-I
1	-	+	+[2,3,4]	+[2(weak),3,4]
2	-	+	+[2,3]	+[2,3,4]
3	-	+	+[3,4]	+[3,4]
4	-	+	+[2,3,4]	+[3,4]
5	-	+	+[2,3,4]	+[2(weak),3,4]
6	-	-	+[2,3,4]	+[2,3,4]
7	-	+ (weak)	+[3,4]	+[3,4]
8	ND	-	-	-
9	ND	-	-	-
10	-	+	+[2,3,4]	+[2,3,4]
11	ND	-	-	-
12	-	-	+[2,3,4]	+[2(weak),3,4]
13	ND	-	-	-
	9/13 (69%)	7/13 (54%)	9/13 (69%)	9/13 (69%)

1: in IML

2: enhanced IR in SGL

3: enhanced IR in SL

4: enhanced IR in hilum

ND: no detected changes

Table 1. Comparative qualitative analysis of the effects of PILO on the densities of the synaptic fields of MCs, MFs and interneurones in the DGs of mice and rats.

No loss of CR-IR cells (presumably MCs) or fibres was detected in mice after PILO treatment. In contrast, a considerable loss of CGRP-IR cells (presumably MCs) and IML was observed in 69% of the PILO-treated rats. 41% and 54% of the PILO-treated mice and rats, respectively, exhibited dramatic increases in Timm's staining in the SGL, while 53% and 69% of the PILO-treated mice and rats displayed dramatically enhanced NPY immunoreactivity throughout the entire DG and the SL, respectively. In both species, the paired comparisons revealed some animals which manifested opposite changes in the SGL, *i.e.* Timm+/NPY- and Timm-/NPY+ bands. A one-to-one correlation was found between the absence of CGRP-IR synaptic field in the IML and the upregulation of the NPY-IR elements. Whereas individual variability in NPY immunoreactivity was observed, its great enhancement in the SL (see NPY+[3]) was a standard phenomenon in the PILO-responsive animals, and might serve as a reliable marker of a substantial change in the neural circuits. Increases in Syn-I and NPY immunoreactivity were seen in parallel in the PILO-responsive rats. Such a coincidence was not observed in the mice.

ND: no detectable changes, Timm+: appearance of zinc-containing ectopic fibres in the SGL, [1]: in the IML, [2]: enhanced NPY-IR in the SGL, [3]: enhanced NPY-IR in the SL, [4]: enhanced NPY-IR in the hilum

Rats. Paired comparisons of the CGRP and NPY immunohistochemistry and the Timm's staining (Table 1.) resulted in a one-to-one correlation between a negative CGRP-IR IML (9/13) and a considerable enhancement of the NPY immunoreactivity in the SL (9/13) (Table 1.). However, the negativity of the CGRP-IR IML did not coincide with the unambiguous change in Timm's staining, *i.e.* in the SGL (7/13) (Table 1.). It is noteworthy that every Timm-positive animal exhibited a loss of CGRP immunoreactivity from the IML. Comparison of the Timm's staining with the immunohistochemistry for NPY yielded results in agreement with CGRP immunostaining; each Timm-positive animal exhibited a dramatic increase in density of the NPY immunoreactivity in the SL. In 2 Timm-positive animals (2/7), the SGL was found to be positive, but contained no enhanced NPY immunoreactivity in this layer, in spite of the strongly IR hilum and SL (see rats № 3 and 7 in Table 1.). Interestingly, 2 rats with NPY-IR SGL proved to be Timm-negative.

3.3.4. Effects of convulsions on the pyramidal cells

Neuronal loss was evaluated by means of NeuN immunostaining in the PILO-responsive animals. No visible changes were observed in the hippocampi of rats and the CFLP mice. However, noticeable reductions were found in the PCs of the Balb/c and NMRI strains. In 3 out of the 7 PILO-responsive Balb/c mice, the number of PCs in the CA3a and CA3b subregions was noticeably reduced (Fig. 12.). No considerable loss of PCs was observed in the remaining CA regions.

In the NMRI strain, the cell loss was more pronounced, 8 out of the 18 PILO-responsive mice displayed patchy neuronal loss in the PC layer of CA1 and CA3 regions. In 3 out of 18 PILO-responsive animals, the marked loss of PCs extended from the CA3a/b to the CA3c subregion (Fig. 12. C). Beside the loss of CA3 PCs, the superior blade of the GC layer was damaged to a large extent in the sclerotic mice (Fig. 12. C).

The vulnerability of the PCs was also investigated in the Wistar rat. Similarly to the CFLP mice, no noticeable changes in their number was found, using NeuN immunostaining.

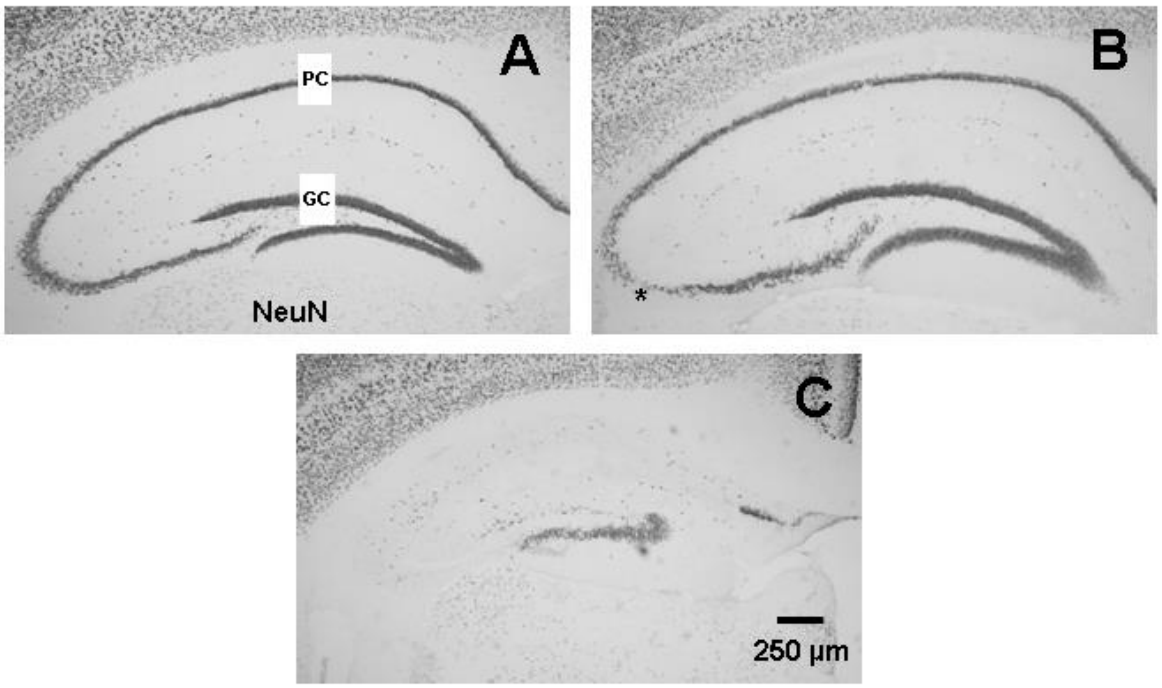

Fig. 12. NeuN immunohistochemistry. High density of NeuN-immunoreactive neurones is visible in the layers of GCs and PCs of the control animals (A). Occasionally, subsets of PCs were lost in patches (asterisk) in the CA3 region (B). NeuN immunohistochemistry confirmed extensive loss of neurones in the sclerotic hippocampus of NMRI mouse (C).
GC: granule cell; PC: pyramidal cell. Scale bar: 250 mm.

3.4. Changes of the iGluRs in the Balb/c and NMRI mice

3.4.1. AMPA receptor subunits

In the control animals, the AMPA receptor (AMPAR) antibodies showed similar immunostaining in the consecutive sections (Fig. 13.). Massive immunostaining was observed with the GluA1 antibody (Fig. 13. A), while the GluA2/3 antibody showed the weakest staining (Fig. 13. E). The antibodies stained mainly fibres and dendrites: the most intense staining was observed in the stratum oriens and stratum radiatum (SR) of the CA1 region. The least intense staining was found in the hilum of the DG and in the SL of the CA3. The GluA2 and GluA2/3 antibodies also stained several multipolar neurones in the hilum (Fig. 13. C, E), which were suggested to be MCs (Tang et al. 2005). It is worth noting that the layer-to-layer analysis of the semiquantitative data of the two mouse strains revealed significant density

differences in the GluA2 immunoreactivities of the DG. The ML and the hilum of the NMRI mice showed lower values compared to the Balb/c mice.

PILO-treatment resulted in remarkable changes of the immunoreactivity, the extent of which was analysed in some of the hippocampal layers by means of semiquantitative immunohistochemistry (Table 2, Fig. 14.). The density of the GluA1 immunoreactivity decreased in every hippocampal layer (Fig. 13. B), except the SR of CA1 of the NMRI mice. In all other layers, very similar changes were observed in both strains. The most significant reductions were found in the dentate hilum (-72% for Balb/c and -69% for NMRI).

The GluA2 immunoreactivity decreased in both strains (Fig. 13. D). The intensity changes in the layers were two- or three-fold higher in the Balb/c strain than in the NMRI strain. The highest reduction of the GluA2 immunoreactivity was found in the synaptic field of the MFs in both strains. The statistical analysis of the GluA2/3 immunohistochemical results (Fig. 13. F) showed largely similar alterations. The lowest density values and the highest degree of reduction of the optical densities were found in the hilum of the DG in the Balb/c and NMRI mice (-58% and -45%, respectively). The optical density of the hilar immunopositive neurones was reduced significantly in both strains (-29% for Balb/c and -62% for NMRI).

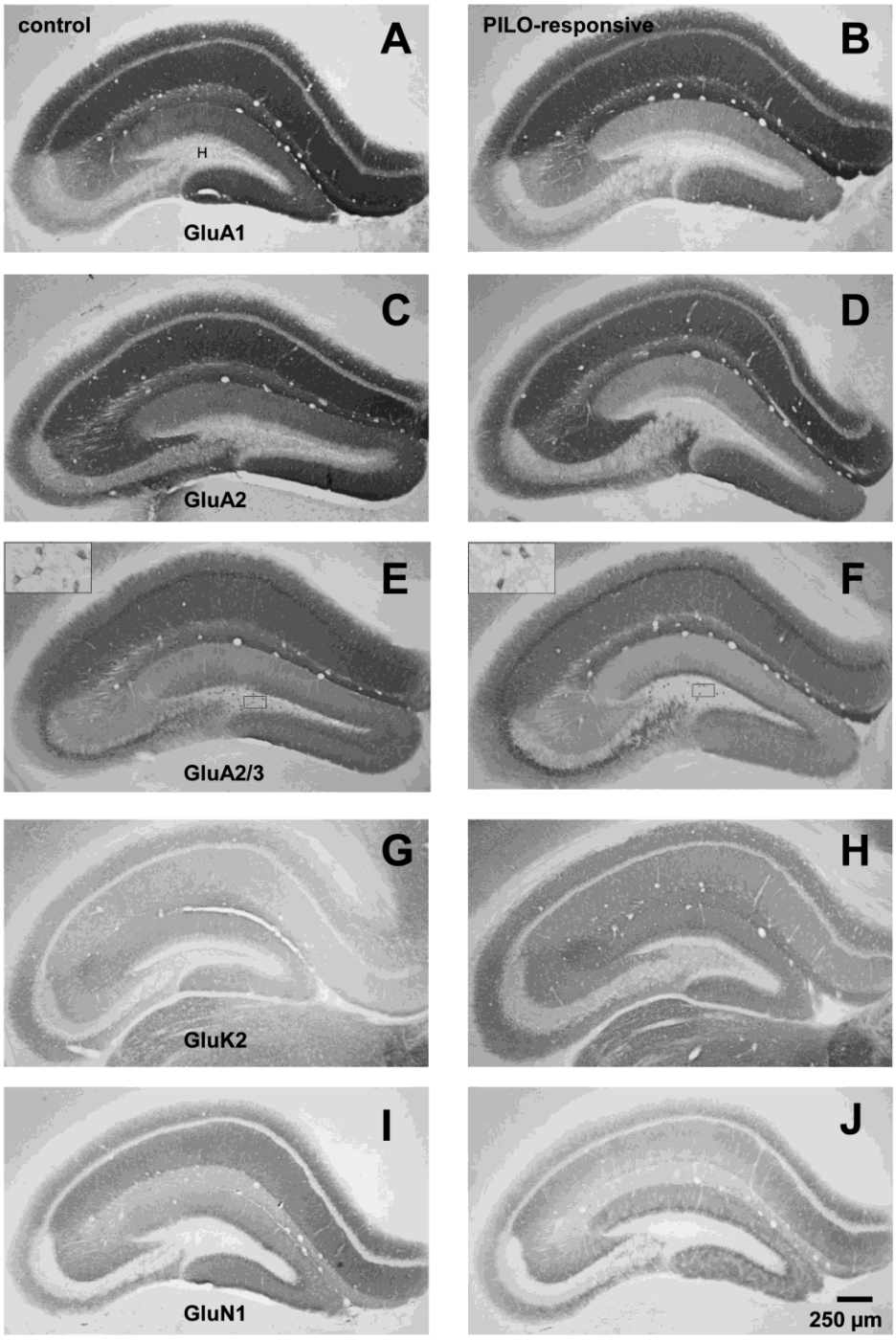

Fig. 13. PILO-treatment resulted in intensity changes in the immunoreactivity for GluA1 (A, B), GluA2 (C, D), GluA2/3 (E, F), GluK2 (G, H) and GluN1 (I, J) in the hippocampal layers of control (A, C, E, G and I) and PILO-responsive (B, D, F, H and J) Balb/c mice. The immunohistochemical results show an overall reduction in the AMPAR subunit- and GluN1-immunoreactive densities, whereas the GluK2 immunoreactivity increases in the whole hippocampus. Note that the spontaneous AMPAR immunoreactivity nearly vanished in the hilar neuropil (compare insets in E and F), while many multipolar neurones, supposedly MCs, retained their immunoreactivity for the AMPAR subunits in the hilum. H: hilum. Scale bar: 250 mm.

3.4.2. NMDA receptor subunits

In the control animals, GluN1 immunohistochemistry displayed a laminar staining pattern in the hippocampus, which was similar to the AMPAR immunostaining (Fig. 13.). In contrast to the AMPAR antibodies, the GluN1 antibody did not stain perikarya in any of the observed areas while massive neuropil labelling was found in the SO and the SR. Moderate immunostaining was experienced in the SLM and the SM, while the weakest staining was observed in the hilum, the SL of CA3 and in the pyramidal and the granular layers.

PILO treatment exerted measurable effects on the GluN1 immunostaining in the hippocampal layers of the two examined mouse strains (Fig. 13. J, Table 2). In the Balb/c animals, the intensity of the staining in the SR and in the SLM of CA1 were significantly decreased (-32% and -36%, respectively, Table 2). The PILO treatment did not cause modification in the immunostaining density of the overall ML of the DG. However, in the close vicinity of the GC layer, that is in the SGL, our semiquantitative method revealed a significant intensity decrease (-16%). In the NMRI mice the only significant change was an increase (+29%), measured in the SLM of CA1.

	Animal strain	SR	SLM	SLM (CA3)	ML	SGL	H	SL
GluA1	Balb/c	-12^{**}			-42^{****}		-72^{****}	-34^{****}
	NMRI	-1			-28^{****}		-69^{****}	-35^{****}
GluA2	Balb/c	-17^{****}			-33^{****}		-64^{****}	-45^{****}
	NMRI	-6^{*}			-18^{**}		-32	-27^{****}
GluA2/3	Balb/c	-9^{**}			-32^{****}		-58^{****}	-14
	NMRI	-3			-21^{**}		-45^{**}	-23^{**}
GluK2	Balb/c	$+23^{***}$		$+15^{*}$	$+13^{*}$		$+43^{*}$	$+6.5$
	NMRI	$+13^{****}$		$+8^{**}$	-3		-27^{**}	$+1$
GluN1	Balb/c	-32^{****}	-36^{****}		-4	-16^{**}		
	NMRI	-2	$+29^{**}$		-0.4	-6		

Table 2. The summary of the effects of PILO treatment on the GluA1, GluA2, GluA2/3, GluK2, GluN1 immunoreactivities in the hippocampal layers of the non-sclerotic Balb/c and NMRI mice. The changes of immunoreactivities are expressed in percent. The values of significance are indicated as follows:

* $p < 0.05$, ** $p < 0.01$, *** $p < 0.001$, **** $p < 0.0001$.

Note the several marked interstrain differences in the responses of the strains to the convulsant at the level of the iGluRs.

SR: stratum radiatum; SLM: stratum lacunosummoleculare; ML: molecular layer; SGL: supragranular layer; H: hilum; SL: stratum lucidum.

3.4.3. Kainate receptor subunits

The application of the rabbit monoclonal antibody to low affinity GluK2 kainate receptor (KAR) subunit resulted in a staining pattern, which was very similar to that of the AMPAR antibodies in the hippocampus (Fig. 13.). In the control animals, strong immunoreactivity was observed in the hippocampus. Weak immunostaining was found in the pyramidal and the granular layers, in the hilum and in the SL of CA3 (Fig. 13. G). The layer-to-layer comparisons of the data from the two strains revealed significant intensity differences in the GluK2 immunoreactivities: the ML and the hilum of the NMRI strain exhibited higher density values than those in the Balb/c mice (+22% and +79%, respectively, empty columns in Fig. 14.).

After PILO treatment, the intensity of the GluK2 immunoreactivity increased in the hippocampus (Fig. 13. H). An increase in the immunostaining density was found in every hippocampal layer of the Balb/c mice: the highest increase was observed in the hilum (+43%; Table 2). The opposite alteration, the decrease of the GluK2 density was observed in the hilar region of the NMRI mice (-27%; Table 2). Intensity increases were also significant in the SR of CA1 and the SLM of CA3 in the Balb/c strain (+23% and +15%, respectively). In the NMRI mice less increase was observed in those layers (+13% in SR, +8% in SLM). The ML of the Balb/c mice showed +13% intensity increase, while no alteration was measured in the ML of the NMRI mice. In both strains, no significant changes were detected in the staining intensity of the SL (Table 2).

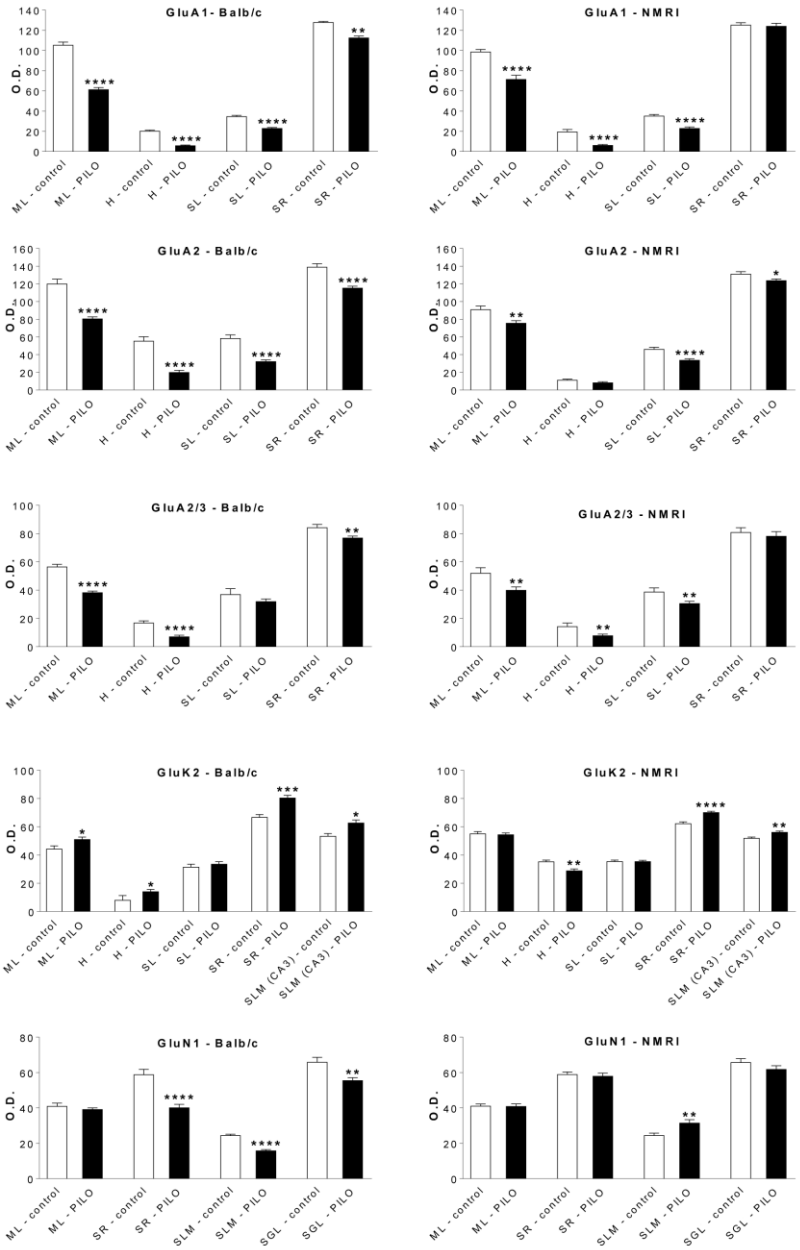

Fig. 14. Distributions of GluA1, GluA2, GluA2/3, GluK2, GluN1 immunoreactivities in the hippocampal layers of control (empty columns) and non-sclerotic PILO-responsive (filled columns) Balb/c and NMRI mice are compared. The most remarkable differences between the two studied strains were found in the GluA2 and GluK2 immunoreactivity of the hilum and the ML (compare the matched empty columns). Note that the PILO treatment resulted in general reductions in the densities of the hippocampal AMPAR and GluN1 subunits, and increases in the levels of the GluK2 immunoreactivity in both strains (empty vs filled columns). (Differences were significant at $p < 0.05$; *$p < 0.05$, **$p < 0.01$, ***$p < 0.001$, ****$p < 0.0001$.) The values of the significant changes are summarized in Table 1.

ML: molecular layer; H: hilum; SL: stratum lucidum; SR: stratum radiatum; SLM: stratum lacunosum-moleculare; SGL: supragranular layer.

4. DISCUSSION

4.1. Synaptic changes in Wistar rat and CFLP mouse hippocampi

4.1.1. Species-dependent changes in the levels of Syn-I

The synapsins are thought to be important molecules in synaptic maturation and in the regulation of the release of neurotransmitters, including Glu (Greengard et al. 1993). High levels of Syn-I gene and protein expression have been found in the hippocampal principal neurones (Melloni et al. 1993). We assumed that these neurones displayed the excessive activities in SE animals, therefore the Syn-I density increased in their hippocampi (especially in the synaptic fields of the sprouted MFs).

The genetic deletion of Syn-I in mice led to a severe epileptic phenotype with recurrent seizures by the age of ~ 2 months (Rosahl et al. 1995). In those Syn-I knock-out animals, the number of synaptic vesicles containing either Glu or GABA decreased, which supports the view that Syn-I plays a controversial role in epileptogenesis (Bogen et al. 2006). The impairment of GABAergic inhibitory transmission was apparently more profound than that of the excitatory neuronal circuits (Baldelli et al. 2007).

The present study demonstrated alterations of the Syn-I expression in some hippocampal areas of the PILO-treated animals. Any change in Syn-I density obviously indicated a disturbance in the balance of the excitatory and inhibitory systems. As we described earlier, contrasting alterations in Syn-I immunoreactivity were found in the three major MF areas of the PILO-treated mice: the expression of Syn-I was increased in the SL, decreased in the hilum and remained unaltered in the SGL (Karoly et al. 2011).

An increase in Syn-I density in the SL is in line with the increases in both Timm's staining and NPY immunoreactivity, indicating the greatly enhanced number of presynaptic axon terminals. The decrease in Syn-I density in the mouse hilum was unexpected, since both the Timm's staining intensity and the NPY immunoreactivity were increased. Moreover, the CR-positive glutamatergic MCs seemed to survive the PILO treatment. Thus, the Syn-I-associated glutamatergic system is presumed to be maintained, or even increased. The reduction in Syn-I implies that a subset(s) of either or both of the major opposite neurotransmission systems was/were downregulated or even lost. The population of GCs has not been reported previously to be subdivided. However, the inhibitory cells are classified

into several groups in the hippocampus, depending on their neuropeptide contents and electrophysiological properties (Freund and Buzsaki 1996).

The strong NPY immunoreactivity suggested that GABAergic horizontal cells (Takács et al. 2008) presumably survived not only in the SL, but also in the hilum of PILO-treated mice. It is well known that there are several other GABAergic cells in this region, some of which, *e.g.* the parvalbumin-containing neurones, have been reported to be reduced in PILO-treated animals (Kobayashi and Buckmaster 2003; Károly et al. unpublished observations). Accordingly, the net decrease of Syn-I density in the hilum might result from the loss or downregulation of a subset of the GABAergic neurones which are assumed to be distinct from the "densely-spiny hippocampal cells projecting to the medial septum" (DSHS cells). Moreover, the increased NPY immunoreactivity in the hilum and SL, which was proportional to the decreased Syn-I immunoreactivity in the hilum, tentatively suggests certain compensatory mechanisms for the loss of a subset of GABAergic cells in the hippocampal neuronal circuitry. This mechanism might not necessarily involve Syn-I-associated neurotransmission.

In contrast with the mice, the PILO treatment of the rats increased the Syn-I density in every hippocampal area where the NPY immunoreactivity was elevated. These changes were positively correlated. It should be noted that the increased density of Syn-I lagged significantly behind that of NPY, which can be accounted for by either the ambiguous changes in the two major opposite neurotransmitter systems during epileptogenesis, or that the possibly increased NPY-mediated transmission may not utilize Syn-I.

4.1.2. GAP-43 immunohistochemistry

The staining pattern of GAP-43 protein in control animals conforms the literature data (Tolner et al, 2003). The GAP-43 immunoreactivity of the IML in the PILO-reacted animals decreased significantly. Our data are in agreement with the after-seizure down-regulation of GAP-43 expression in the IML (Borges et al, 2004; Longo et al, 2005; Tolner et al, 2003). Other studies reported the upregulation of this protein after kainic acid treatment (McNamara and Routtenberg, 1995), kindling (Dalby et al, 1995) or PILO seizures (Naffah-Mazzacoratti et al, 1999). In embryonic stem cell cultures, GAP-43 production was restricted to a separate axonal compartment (Mundigl et al, 1993). GAP-43 was expressed transiently by the

dendrites as well, but the main localization site was in the axonal growth cone (Goslin and Banker, 1990). GAP-43 protein is presynaptic (Skene et al, 1986), but we do not know whether it localizes in axon terminals after the sprouting: our results suggest, that following sprouting GAP-43 disappears from the sprouted terminals. No change of GAP-43 staining was noted in human non-sclerotic, epileptic hippocampi in the molecular layer of the DG (Proper et al, 2000). In other epilepsy cases with hippocampal sclerosis elevated GAP-43 level was measured in the supragranular layer of the DG (Proper et al, 2000). In our study, there was a considerable loss of GAP-43 immunostaining in the IML of both CFLP mice and rats (Károly et al, 2011). The decreased GAP-43 staining means that GAP-43 may not be an essential component of the sprouted presynaptic axons in chronic PILO seizures.

4.2. Interneuronal changes in the murine hippocampus

4.2.1. Increased NPY immunoreactivity

The hippocampal distribution of NPY-IR neuronal cell bodies is well documented (Gall et al. 1990, Haas et al. 1987, Kohler et al. 1986) in both rodent species. In the control animals, the highest level of this neuroactive substance is found in the SLM, but scattered interneurones are present throughout the hippocampus.

Marked changes in the distribution pattern of NPY immunoreactivity in PILO-treated species were reported by Lurton and Cavalheiro (1997), Nadler et al. (2007), Scharfman and Gray (2006) and Winawer et al. (2007): intense staining in the synaptic fields of the MFs, *i.e.* the hilum and SL and variable immunoreactivity in the SGL were observed. The authors also agreed on the strong enhancement of NPY immunoreactivity in the interneurones throughout the hippocampus.

Two major sources of the elevated NPY level may be supposed: (1) an unnatural appearance of NPY in the GCs, and (2) the increased activity of the interneurones. (1) The *de novo* synthesis of NPY mRNA and NPY in the GCs has been reported (Gall et al. 1990, McCarthy et al. 1998). Several experiments have shown that tonic-clonic seizures evoked by electrical kindling (Rizzi et al. 1993), kainate (Gruber et al. 1994, Sperk et al. 1992) and PILO (Lurton and Cavalheiro 1997) result in strongly elevated NPY immunoreactivity in the MF field, which persists for months. (2) NPY and its mRNA levels are also markedly increased in the hippocampal interneurones (Gall et al. 1990, Marksteiner et al. 1990, Sperk et al. 1992).

The above experiments revealed that the NPY immunostaining is enhanced in the outer molecular layer, where these neurones richly arborize.

Further investigations showed that the two different sources of NPY elevation displayed different time-course changes after the SE. In kainate SE (Gruber et al. 1994), both cell groups responded with rapid expression of NPY mRNA, but whereas the NPY mRNA level soared to ~ 60-fold in the GCs after 24 h, the increase in the hilar interneurones was only 2-fold. During the next 24 h, the level of NPY mRNA in the GCs dropped to the control values, while the NPY mRNA in the hilar interneurones increased further. Four months after the SE, the NPY mRNA in the GCs remained at a very low level, while in the interneurones it rose further on to more than 10 times of the control values.

Earlier papers on the changes of limbic NPY after SE (Lurton and Cavalheiro 1997, Scharfman and Gray 2006, Winawer et al. 2007) ascribed the elevated levels of NPY in the hilum, the SL and the SGL directly to the activated GCs. Strikingly, NPY immunoreactivity within the GCs was not described at any examined time point of the post-treatment period in any of the papers, in contrast with that in the interneurones, which was observed to be intense. Yet, the GCs have been so far considered responsible for the massive NPY-IR immunostaining in the terminal field of the MFs (Nadler et al. 2007).

Different populations of NPY-IR interneurones have been described in the DG (Deller and Léránth 1990). The GABAergic neurones, in which NPY and somatostatin were colocalized, displayed horizontal dendrites and were named spiny GABAergic cells (Acsády et al. 1998). These interneurones were further classified as hippocamposeptal neurones by Gulyás et al. (2003). Although, NPY immunohistochemistry was not applied, possibly the same cell type was further characterized by Takács et al. (2008) as a subclass of GABAergic neurones which exhibit densely-spiny horizontal dendrites restricted to the hilum and SL, and established synapses in the septum. They coined this cell type DSHS cells. Direct evidence is not yet available concerning that the DSHS cells express NPY, but all lines of evidence together strongly suggest that these cells might be responsible for the dramatic increase in NPY immunoreactivity in the hilum and SL of the chronic Timm-positive animals. Thus, the DSHS cells might be among those which react to PILO treatment most intensely and early with increased NPY expression, and the DSHS cells could therefore play an important role in the process of epileptogenesis.

In view of the general inhibitory functions of NPY as a neuromodulator substance on the postsynaptic cells, the synergistic actions of GABA and co-released NPY might have a protective role (Colmers and Bahh 2003). This postulated mechanism, however, should not be totally effective for the principal neurones, since epileptogenesis is a chronic disease in the model animals, and the spontaneous seizures result in slowly progressing neuronal degeneration.

Analogously to the appearance of NPY immunoreactivity in the SL, the newly appeared NPY immunostaining in the SGL could not be explained by the ectopic MFS of the activated GCs. Direct evidence is not yet available, but the supragranular staining could be attributable to hilar interneurones, in which the seizures could induce axonal sprouting into the SGL to establish inhibitory axo-dendritic or axo-axonic connections on the proximal dendrites or on the ectopic MFs of the GCs, respectively. Our present theory is supported by the ectopic sprouting of GABAergic interneurones into the SGL, which has been reported in the mouse model of TLE (Zhang et al. 2009).

4.2.2. MFS versus enhanced NPY immunostaining as markers of epileptogenesis

The role of MFS in epileptogenesis has been debated, since spontaneous recurrent seizures could be evoked without the appearance of MFS in the PILO model of epilepsy and the kainate model of TLE (Longo and Mello 1997, Longo and Mello 1998). Nevertheless, most researchers seem to agree that MFS, and especially ectopic MFS in the SGL, is a prerequisite for recurrent spontaneous convulsions, and they have often used Timm's staining as morphological evidence of the ongoing epileptogenesis.

Robust upregulation of hippocampal NPY is an accepted marker for seizures (Sperk et al. 1992, Vezzani et al. 2002, 2004). Our comparative studies of Timm's staining and NPY immunostaining on the consecutive sections indicated that zinc histochemistry in one-fifth of mice and rats failed to highlight animals which may have suffered from spontaneous convulsions. We therefore suggest that NPY immunohistochemistry might be more reliable for confirmation of the ongoing epileptic activity in these two rodent species.

4.3. Effects of seizures on principal neurones

4.3.1. Changes of mouse and rat mossy cells following PILO treatment

It is widely accepted that two main classes of hilar neurones can be distinguished: (1) the glutamatergic MCs (Scharfman 1995, Soriano and Frotscher 1994), and (2) various subclasses of GABAergic neurones (for a review see Freund and Buzsáki 1996).

There have been different reports as to whether the MCs are lost in the TLE or whether they survive the seizures. Studies of this question in the human disease and in animal models indicated that in several pathological states there is a selective and dramatic cell loss in the hilum, and the MCs are susceptible to the seizures (Babb et al. 1984, Margerison and Corsellis 1966, Mathern et al. 1997). Loss of the MCs has generally been accepted as coincident with the hyperexcitability of the GCs, which inspired the "dormant basket cell" hypothesis (Buckmaster and Jongen-Rélo 1999; Longo et al. 2003; Sloviter 1991).

4.3.1.1. Mouse mossy cells

In our studies, three mouse strains were compared for their chronic responses to the chemoconvulsant PILO. According to the historical records (Beck et al. 2000; Chia et al. 2005) about the origins of CFLP, Balb/c and NMRI strains, no common ancestors of these strains were found.

With the using of CR and GluR2/3 immunohistochemistry no changes were observed in the number and distribution of CR-IR hilar perikarya, 96% of which have been supposed to be MCs (Blasco-Ibanez and Freund 1997, Liu et al. 1996) in the CFLP mice. Our findings on the MCs of the CFLP strain are in sharp contrast with the general and widely accepted concept that the MCs are highly vulnerable to glutamate-mediated seizures. SE induced by convulsants such as PILO (Silva and Mello 2000) and kainate (Volz et al. 2011) led to a loss of MCs. However, in two other mouse strains (Balb/c and NMRI) lacking documented common ancestors (Beck et al. 2000) with the CFLP strain, we also found dramatic and different reductions in the density of the MCs after PILO treatment (Dobó et al. 2015).

Despite the partial loss of MCs in the Balb/c and NMRI mice, we did not find reduction in the CR immunoreactivity in the IML in any of the studied strains. This is probably due to the limited power of the semi-quantitative measurements of the highly

superimposed dense axon terminals, which is certainly the case for Balb/c and NMRI mice, as well. The lack of changes after the fornix lesion in the mouse proved that the vast majority of the immunostaining in the IML could be ascribed to the MCs, and not to the supramamillo-hippocampal pathway, which could have been supposed by the reports on this pathway in monkeys (Nitsch and Leranth 1993).

MFS has previously been detected in the epileptic hippocampus by means of Timm's method (Cavalheiro et al. 1996, Jiao and Nadler 2007, Lemos and Cavalheiro 1995). Our findings corroborate the earlier literature data on the increased density of MFs in PILO-treated animals and the appearance of ectopic MFs in the SGL.

Similar distribution patterns of the zinc-containing elements were found in the control and the Timm-positive animals, which correlated with the CR immunohistochemistry. The only slight, but still remarkable difference was the persistence of Timm's staining in the outer zone of the IML of the Timm-positive mice (Fig. 3 D). Since this layer has been reported to receive synaptic inputs typically from the glutamatergic MCs (Buckmaster et al. 1992, 1996, Laurberg and Sorensen 1981, Ribak et al. 1985, Swanson et al. 1978, Zimmer 1971), the persistence of the zinc content of the layer indicated survival of the MCs. This seems to be contradictory to the findings of Silva and Mello (2000), who demonstrated that PILO-induced epileptic seizures eliminated the CR-IR axons of the MCs from the IML.

In summary, our experiments indicate that the MCs of the CFLP mouse may not be as vulnerable as those in the Balb/c and NMRI strains. This statement is implicitly confirmed by several lines of evidence: no reduction in (1) the CR-IR perikarya in the hilum, (2) the CR-IR axons in the IML, or (3) the zinc-containing elements in the IML, and (4) a lack of noticeable CR-IR input through the fornix.

4.3.1.2. Rat mossy cells

Only few slightly labelled CGRP-IR cells remained in the DG in the PILO-treated rats. Moreover, the immunoreactivity vanished from the IML. The question then arises as to whether these cells died, or just lost their immunoreactivity for CGRP, indicating altered electrophysiological properties as supposed by Scharfman et al. (2001).

The application of CGRP immunohistochemistry and Timm's staining on consecutive sections from control rats pointed to similar layers with comparable widths in the IML. The

pale zinc staining in the IML could therefore be attributed to the axon varicosities of the glutamatergic MCs, which is in line with the synaptic field of the MCs (Buckmaster et al. 1992, Buckmaster et al. 1996, Laurberg and Sorensen, 1981; Ribak et al. 1985, Swanson et al. 1978, Zimmer 1971). Zinc exerts pharmacological effects locally on the NMDA receptors and Glu transporters (Paoletti et al. 2009). Nevertheless, whether zinc is a proconvulsant (Pei et al. 1983) or an anticonvulsant remains unclear (Paoletti et al. 2009, Williamson and Spencer 1995). In every Timm-positive rat, in which ectopic MFs appeared in the IML as a narrow band (*i.e.* the SGL), the Timm-positive staining, indicative of glutamatergic neurotransmission, vanished from the remainder of the IML, and the CGRP immunoreactivity disappeared from its whole width. Therefore, even if the MCs had survived the seizures, they would have been converted into silent neurones losing their CGRP content.

4.3.2. Effects of seizures on pyramidal cells

Several lines of evidence suggest the vulnerability of PCs in conclusions (Wasterlain *et al.* 1993; Borges *et al.* 2003). The question whether the loss of cells contributed to the epileptogenesis or the cell loss was the consequence of the recurrent seizures is still debated.

Different rodent models are useful for the investigation of complex neurological disorders such as epilepsy. Extrapolation of the results from one species and/or strain to others, is fairly questionable, since the murids demonstrate significant species-, strain- and even intrastrain differences in the susceptibility to convulsive agents and the consequences of seizures (Curia *et al.* 2008; Portelli *et al.* 2009).

Various rodent strains exhibit high resistence to chemically induced SE, and display no degeneration or cell damage in spite of seizures (Schauwecker and Steward 1997). For example, the treatment with PILO did not result in noticable loss in the PCs of the Wistar rats suffering from recurrent seizures (Dobó et al. 2015).

We found important differences in the vulnerability of the PCs among the three studied mouse strains. While no loss of PCs was noticed in the PILO-responsive CFLP mice, the PCs of Balb/c and NMRI suffered damage after the seizures. There was a considerable elimination of PCs in CA3c in 17% of the PILO-responsive NMRI, whereas these cells seemed to remain intact in the Balb/c mice. This difference is in line with several papers reporting that (1) Balb/c-related strains were found to be resistant to PILO-induced SE

(Schauwecker 2012), and (2) the descendants of the so called Swiss mice, a separate genealogical line (Beck et al. 2000), including the NMRI strain, were found to suffer severe damage to the CA3 PCs (Turski et al. 1984; Riban et al. 2002; Tang et al. 2005).

According to our observations, the CA1 and CA3a PCs seemed to be the most vulnerable, while the CA3c PCs seemed to be the most resistant to the recurrent convulsions. The high resistance of the PCs in CFLP and the total disappearance of the PCs from sclerotic NMRI mice fundamentally question the role of PCs in either the epileptogenesis or in the chronic seizure activity.

4.4. Changes of the density of the iGluRs in the Balb/c and NMRI mice

4.4.1. The AMPA receptor subunits

The semiquantitative layer-to-layer comparisons of the AMPAR subunits exhibited interstrain differences between the age-matched control animals as to the GluA2 subunit. No differences were seen in the density of the GluA1 subunit. The differences were confined to the DG; the hilum contained less GluA2 (-79%) in the NMRI mice compared to the Balb/c. Coincidentally, the NMRI strain received higher dose of injected PILO than the Balb/c strain to obtain the same number of PILO-responsive animals. Since the hilar GluA2 immunoreactivity is accounted for by the MCs, the remarkably higher density of the calcium impermeable GluA2 subunit in the Balb/c mouse may serve as an explanation for the higher vulnerability to PILO compared to the NMRI strain animal.

After the PILO treatment, our AMPAR immunohistochemical results showed an overall decrease in the density of this iGluR type in the non-sclerotic PILO-responsive hippocampus. It was described earlier that the experimental inhibition of AMPARs can prevent long-term increases in seizure susceptibility and seizure-induced neuronal injury (Koh et al. 2004). Therefore, the appreciable decrease of AMPARs of the PILO-responsive mice suggested an extensive attenuation of the excitatory response to glutamate.

4.4.2. The NMDA receptor: GluN1 subunit

NMDA receptors (NMDARs) colocalize with AMPARs to establish functional postsynaptic channel complexes in glutamatergic synapses in the central nervous system. The NMDARs can modulate neurotransmission by generating long-lasting Ca^{2+} influx and depolarization.

The functional channels are heteromeric, containing the obligatory GluN1 and the associated other subunits of any of the NR2A-D subtypes (Garcia-Gallo *et al.* 2001).

The studied mouse strains expressed different levels of the GluN1 subunit. In Balb/c mice, significant decrease was detected in the apical dendritic area of CA1 PCs: reductions were found in the SR, where the Schaffer collaterals terminate, and in the SLM (-32% and -36%, respectively), where many axons of the temporo-ammonic pathway innervate the distal dendritic branches of PCs. The reduction in the CA1 may result from the downregulation of the NMDARs, which was reported in electroconvulsive experiments (Park et al. 2014). The significance of the downregulation is unclear, but a neuroprotective role can be supposed (Soriano et al. 2006, Paoletti and Neyton 2007).

Similar reduction in the SR and SLM may be accounted for by either the lack of precise membrane trafficking of the NMDAR subunits to input-specific sites along the dendritic tree, or involvement of the epileptic discharges in CA1 PCs located in the terminal field of the two axonal systems: the perforant pathway–MF–Schaffer collateral axis and the temporo–ammonic pathway. The decrease of GluN1 in the SGL may be attributed to the appearance of the ectopic MFs in this sublayer (Buckmaster 2012; Pierce et al. 2005).

The significant increase of the GluN1 immunoreactive density in the SLM of CA1 might have contributed to the higher sensibility of the NMRI strain to the PILO-induced hippocampal sclerosis.

4.4.3. The low-affinity kainate receptor subunit: GluK2 subunit

KARs are located on both sides of the synapse, where they play various roles (Huettner, 2003; Lerma, 2003; Fernandes et al, 2009; Sihra et al, 2014). In our experiments, the GluK2 subunit was used to show the distribution of the KARs by means of immunohistochemistry. This subunit was suggested to play an important role in the formation of both presynaptic and postsynaptic KARs (Wenthold et al, 1994; Contractor et al, 2001). In the control animals, interstrain differences were restricted to the DG: the ML and the hilum of the NMRI mice contained +22% and +79% more immunoreactivity, respectively, than those of the Balb/c strain. Investigation of GluK2-overexpressing and knockout animals suggested that the presence of hippocampal GluK2 promotes seizure activity (Mulle et al, 1998; Telfeian et al, 2000). Although the optical densities of the AMPARs were found to be generally decreased in

the non-sclerotic PILO-responsive animals in both mouse strains, immunolabelling for the GluK2 was ambiguously altered between the two strains and between the hippocampal layers within the given strain. In Balb/c mice, the decrease of AMPARs was accompanied by the increase of KAR immunoreactivity in the DG. In the NMRI mice, AMPAR decreases were not followed by opposite KAR alterations. The diverse changes in the GluK2 levels within the individual hippocampal layers cannot be interpreted reliably on the basis of the data available in the literature (Vincent and Mulle, 2009). The GluK2 mRNA is mainly expressed in the principal neurones of the hippocampus (Paternain et al, 2000). Presynaptic GluK2-containing KARs can modulate Glu release not only via ionotropic but also via metabotropic ways (Rodriguez- Moreno and Sihra, 2007). Furthermore, Glu may exert bimodal effect on its own release in a concentration dependent manner on certain presynaptic elements (Ruiz and Kullmann, 2012). The net effects of the GluK2-associated changes on the spontaneous recurrent seizures may also be affected by the GABAergic interneurones, which may receive glutamatergic inputs, and are involved in the regulation of the activity of the hippocampal principal cells (Christensen et al, 2004).

5. CONCLUSIONS

In a rodent model of epilepsy, similar treatments of rats and mice with PILO induce comparable behavioural patterns and repeated episodes of chronic spontaneous seizures. The hippocampi of these PILO-treated animals were analysed by means of a novel combination of zinc histochemistry and immunohistochemistry for certain neuronal markers.

(1) Important interspecies differences were found during the epileptogeneses of the rat and the mouse in the PILO model.

(a) The hilar MCs are more vulnerable in rats than in mice.

(b) The higher damage is accompanied by the more intense ectopic sprouting of the GCs.

(2) Differences in predispositions to PILO-induced neuronal alterations were found in mouse strains.

(a) The MCs of the CFLP seemed to resist the effect of PILO, whereas these cells of NMRI mice were found to be highly susceptible to the same treatment.

(b) A remarkably lower density of the calcium impermeable GluA2 subunit was revealed in hilum of the NMRI than of the Balb/c mice.

(3) PILO-induced chronic seizures resulted in significant alterations of the patterns of the iGluR subunits in mouse strains. The alterations of the neuronal circuitry showed bidirectional relationships with the inversely correlated changes of the GluA1 and GluA2 levels in the DG of the individual NMRI mice.

(4) Our collated results showed that NPY immunohistochemistry may be the most sensitive and reliable for visualisation of the epileptic processes in each tested murine strains.

6. ACKNOWLEDGEMENTS

Firstly, I would like to thank my supervisors Prof. Dr. András Mihály and Dr. Endre Dobó for continuous support of my research work. Prof. Mihály provided me an excellent opportunity to join his team, and gave access to the laboratory and research facilities. I am grateful to Dr. Dobó for his patience, insightful comments and encouragement. My sincere thanks also goes to Dr. Ibolya Török for brainstorming discussions and her guidance in the laboratory work. I also remain indebted to Beáta Krisztin-Péva for her invaluable help at the statistical analyses.

I would like to express my sincere gratitude to Ms Mónika Kara, Ms Katalin Lakatos, Ms Andrea Kobolák for the precise technical assistance. I would also like to take this opportunity to thank Ms Hajnalka Vékony for the painstaking animal husbandry.

Last but not least, my special thanks goes to my family.

Grant: TÁMOP 4.2.2-A-11/1/KONV-2012-0052.

REFERENCES

Acsady L, Kamondi A, Sik A, Freund T, Buzsaki G (1998) GABAergic cells are the major postsynaptic targets of mossy fibers in the rat hippocampus. J Neurosci 18:3386-3403.

Amaral DG (1978) A Golgi study of cell types in the hilar region of the hippocampus in the rat. J Comp Neurol 182:851-914.

Babb TL, Brown WJ, Pretorius J, Davenport C, Lieb JP, Crandall PH (1984) Temporal lobe volumetric cell densities in temporal lobe epilepsy. Epilepsia 25:729-740.

Baldelli P, Fassio A, Valtorta F, Benfenati F (2007) Lack of synapsin I reduces the readily releasable pool of synaptic vesicles at central inhibitory synapses. J Neurosci 27:13520-13531.

Baude A, Nusser Z, Roberts JD, Mulvihill E, McIlhinney RA, Somogyi P (1993) The metabotropic glutamate receptor (mGluR1 alpha) is concentrated at perisynaptic membrane of neuronal subpopulations as detected by immunogold reaction. Neuron 11:771-787.

Beck JA, Lloyd S, Hafezparast M, Lennon-Pierce M, Eppig JT, Festing MF, Fisher EM (2000) Genealogies of mouse inbred strains. Nat Genet 24:23-25.

Ben-Ari Y (1985) Limbic seizure and brain damage produced by kainic acid: mechanisms and relevance to human temporal lobe epilepsy. Neuroscience 14:375-403.

Benowitz LI, Rodriguez WR, Neve RL (1990) The pattern of GAP-43 immunostaining changes in the rat hippocampal formation during reactive synaptogenesis. Brain Res Mol Brain Res 8(1):17-23.

Blasco-Ibanez JM, Freund TF (1997) Distribution, ultrastructure, and connectivity of calretinin-immunoreactive mossy cells of the mouse dentate gyrus. Hippocampus 7:307-320.

Bogen IL, Boulland JL, Mariussen E, Wright MS, Fonnum F, Kao HT, Walaas SI (2006) Absence of synapsin I and II is accompanied by decreases in vesicular transport of specific neurotransmitters. J Neurochem 96:1458-1466.

Borges K, Gearing M, McDermott DL, Smith AB, Almonte AG, Wainer BH (2003) Neuronal and glial pathological changes during epileptogenesis in the mouse pilocarpine model. Exp. Neurol. 182 (1), 21–34.

Borges K, McDermott DL, Dingledine R (2004) Reciprocal changes of CD44 and GAP-43 expression in the dentate gyrus inner molecular layer after status epilepticus in mice. Exp Neurol 188(1):1-10.

Borhegyi Z, Leranth C (1997) Distinct substance P- and calretinin-containing projections from the supramammillary area to the hippocampus in rats; a species difference between rats and monkeys. Exp Brain Res 115:369-374.

Buckmaster PS, Jongen-Relo AL (1999) Highly specific neuron loss preserves lateral inhibitory circuits in the dentate gyrus of kainate-induced epileptic rats. J Neurosci 19:9519-9529.

Buckmaster PS, Strowbridge BW, Kunkel DD, Schmiege DL, Schwartzkroin PA (1992) Mossy cell axonal projections to the dentate gyrus molecular layer in the rat hippocampal slice. Hippocampus 2:349-362.

Buckmaster PS, Wenzel HJ, Kunkel DD, Schwartzkroin PA (1996) Axon arbors and synaptic connections of hippocampal mossy cells in the rat in vivo. J Comp Neurol 366:271-292.

Buckmaster PS (2012) Mossy Fiber Sprouting in the Dentate Gyrus. Jasper's Basic Mechanisms of the Epilepsies [Internet]. 4th edition. Bethesda (MD): National Center for Biotechnology Information (US)

Casoli T, Spagna C, Fattoretti P, Gesuita R, Bertoni-Freddari C (1996) Neuronal plasticity in aging: a quantitative immunohistochemical study of GAP-43 distribution in discrete regions of the rat brain. Brain Res 714(1-2):111-117.

Cavalheiro EA, Santos NF, Priel MR (1996) The pilocarpine model of epilepsy in mice. Epilepsia 37:1015-1019.

Chia R, Achilli F, Festing MF, Fisher EM (2005) The origins and uses of mouse outbred stocks. Nat. Genet. 37 (11), 1181–1186.

Christensen JK, Paternain AV, Selak S, Ahring PK, Lerma J (2004) A mosaic of functional kainate receptors in hippocampal interneurons. J Neurosci, 24(41), 8986-8993.

Colmers WF, El Bahh B (2003) Neuropeptide Y and Epilepsy. Epilepsy Curr 3:53-58.

Colmers WF, Lukowiak K, Pittman QJ (1988) Neuropeptide Y action in the rat hippocampal slice: site and mechanism of presynaptic inhibition. J Neurosci 8:3827-3837.

Contractor A, Swanson G, Heinemann SF (2001) Kainate receptors are involved in short- and

long-term plasticity at mossy fiber synapses in the hippocampus. Neuron, 29(1), 209-216.

Curia G, Longo D, Biagini G, Jones RS, Avoli M, (2008) The pilocarpine model of temporal lobe epilepsy. J. Neurosci. Methods 172 (2), 143–157.

Dalby NO, Rondouin G, Lerner-Natoli M (1995) Increase in GAP-43 and GFAP immunoreactivity in the rat hippocampus subsequent toperforant path kindling. J Neurosci Res 41:613–9

Dani JW, Armstrong DM, Benowitz LI (1991) Mapping the development of the rat brain by GAP-43 immunocytochemistry. Neuroscience 40(1):277-287.

Danscher G, Stoltenberg M, Bruhn M, Sondergaard C, Jensen D (2004) Immersion autometallography: histochemical in situ capturing of zinc ions in catalytic zinc-sulfur nanocrystals. J Histochem Cytochem 52:1619-1625.

Deller T, Katona I, Cozzari C, Frotscher M, Freund TF (1999) Cholinergic innervation of mossy cells in the rat fascia dentata. Hippocampus 9:314-320.

Deller T, Leranth C (1990) Synaptic connections of neuropeptide Y (NPY) immunoreactive neurons in the hilar area of the rat hippocampus. J Comp Neurol 300:433-447.

Dobo E, Torok I, Mihaly A, Karoly N, Krisztin-Peva B (2015) Interstrain differences of ionotropic glutamate receptor subunits in the hippocampus and induction of hippocampal sclerosis with pilocarpine in mice. J Chem Neuroanat 64-65:1-11.

Falconer MA (1974) Mesial temporal (Ammon's horn) sclerosis as a common cause of epilepsy. Aetiology, treatment, and prevention. Lancet 2(7883):767-70

Fernandes HB, Catches JS, Petralia RS, Copits BA, Xu J, Russell TA (2009) High-affinity kainate receptor subunits are necessary for ionotropic but not metabotropic signaling. Neuron, 63(6), 818-829.

Franklin KBJ, Paxinos G (1997) The mouse brain in stereotaxic coordinates. Academic Press, San Diego.

Freund TF, Buzsaki G (1996) Interneurons of the hippocampus. Hippocampus 6:347-470.

Freund TF, Hajos N, Acsady L, Gorcs TJ, Katona I (1997) Mossy cells of the rat dentate gyrus are immunoreactive for calcitonin gene-related peptide (CGRP). Eur J Neurosci 9:1815-1830.

Frotscher M, Seress L, Schwerdtfeger WK, Buhl E (1991) The mossy cells of the fascia dentata: a comparative study of their fine structure and synaptic connections in rodents and primates. J Comp Neurol 312(1):145-163.

Gall C, Lauterborn J, Isackson P, White J (1990) Seizures, neuropeptide regulation, and mRNA expression in the hippocampus. Prog Brain Res 83:371-390.

Garcia-Gallo M, Renart J, Diaz-Guerra M (2001) The NR1 subunit of the N-methyl-D-aspartate receptor can be efficiently expressed alone in the cell surface of mammalian cells and is required for the transport of the NR2A subunit. Biochem J, 356(Pt 2), 539-547.

Goslin K, Schreyer DJ, Skene JH, Banker G (1988) Development of neuronal polarity: GAP-43 distinguishes axonal from dendritic growth cones. Nature 336(6200):672-674.

Goslin K, Banker G (1990) Rapid changes in the distribution of GAP-43 correlate with the expression of neuronal polarity during normal development and under experimental conditions. J Cell Biol;110:1319–31.

Greengard P, Valtorta F, Czernik AJ, Benfenati F (1993) Synaptic vesicle phosphoproteins and regulation of synaptic function. Science 259:780-785.

Gruber B, Greber S, Rupp E, Sperk G (1994) Differential NPY mRNA expression in granule cells and interneurons of the rat dentate gyrus after kainic acid injection. Hippocampus 4:474-482.

Gulyas AI, Hajos N, Katona I, Freund TF (2003) Interneurons are the local targets of hippocampal inhibitory cells which project to the medial septum. Eur J Neurosci 17:1861-1872.

Haas HL, Hermann A, Greene RW, Chan-Palay V (1987) Action and location of neuropeptide tyrosine (Y) on hippocampal neurons of the rat in slice preparations. J Comp Neurol 257:208-215.

Haug FM (1967) Electron microscopical localization of the zinc in hippocampal mossy fibre synapses by a modified sulfide silver procedure. Histochemie 8(4):355-68

Huettner JE (2003) Kainate receptors and synaptic transmission. Prog Neurobiol, 70(5), 387-407

Jiao Y, Nadler JV (2007) Stereological analysis of GluR2-immunoreactive hilar neurons in the pilocarpine model of temporal lobe epilepsy: correlation of cell loss with mossy fiber sprouting. Exp Neurol 205:569-582.

Karoly N, Mihaly A, Dobo E (2011) Comparative immunohistochemistry of synaptic markers in the rodent hippocampus in pilocarpine epilepsy. Acta Histochem 113:656-662.

Karoly N, Dobo E, Mihaly A (2015) Comparative immunohistochemical study of the effects of pilocarpine on the mossy cells, mossy fibres and inhibitory neurones in murine dentate gyrus. Acta Neurobiol Exp 75(2):220-237.

Kienzler F, Norwood BA, Sloviter RS (2009) Hippocampal injury, atrophy, synaptic reorganization, and epileptogenesis after perforant pathway stimulation-induced status epilepticus in the mouse. J Comp Neurol 515:181-196.

Kobayashi M, Buckmaster PS (2003) Reduced inhibition of dentate granule cells in a model of temporal lobe epilepsy. J Neurosci 23:2440-2452.

Koh S, Tibayan FD, Simpson JN, Jensen, FE (2004). NBQX or topiramate treatment after perinatal hypoxia-induced seizures prevents later increases in seizure-induced neuronal injury. Epilepsia, 45(6), 569-575

Kohler C, Eriksson L, Davies S, Chan-Palay V (1986) Neuropeptide Y innervation of the hippocampal region in the rat and monkey brain. J Comp Neurol 244:384-400.

Kopniczky Zs, Dobó E, Borbély S, Világi I, Détári L, Krisztin-Péva B, Bagosi A, Molnár E, Mihály A (2005) Entorhinal cortex lesions rearrange afferents, glutamate receptors, increase seizure latency and suppress seizure-induced c-*fos* expression in the hippocampus of adult rat. Journal of Neurochemistry, 95, pp. 111–124

Korzhevskii DE, Gilyarov AV (2010) Immunocytochemical detection of tissue antigens after prolonged storage of specimens in methylsalicylate. Neurosci Behav Physiol 40(1):107-109.

Kurschner VC, Petruzzi RL, Golden GT, Berrettini WH, Ferraro TN (1998) Kainate and AMPA receptor binding in seizure-prone and seizure-resistant inbred mouse strains. Brain Res. 780 (1), 1–8.

Laurberg S, Sorensen KE (1981) Associational and commissural collaterals of neurons in the hippocampal formation (hilus fasciae dentatae and subfield CA3). Brain Res 212:287-300.

Lemos T, Cavalheiro EA (1995) Suppression of pilocarpine-induced status epilepticus and the late development of epilepsy in rats. Exp Brain Res 102:423-428.

Leranth C, Frotscher M (1989) Organization of the septal region in the rat brain: cholinergic-GABAergic interconnections and the termination of hippocampo-septal fibers. J Comp Neurol 289:304-314.

Lerma, J. (2003). Roles and rules of kainate receptors in synaptic transmission. Nat Rev Neurosci, 4(6), 481-495.

Lewis PR, Shute CC, Silver A (1967) Confirmation from choline acetylase analyses of a massive cholinergic innervation to the rat hippocampus. J Physiol 191:215-224.

Liu Y, Fujise N, Kosaka T (1996) Distribution of calretinin immunoreactivity in the mouse dentate gyrus. I. General description. Exp Brain Res 108:389-403.

Longo B, Vezzani A, Mello LE (2005) Growth-associated protein 43 expression in hippocampal molecular layer of chronic epileptic rats treated with cycloheximide. Epilepsia 46(Suppl 5):125–8

Longo B, Covolan L, Chadi G, Mello LE (2003) Sprouting of mossy fibers and the vacating of postsynaptic targets in the inner molecular layer of the dentate gyrus. Exp Neurol 181:57-67.

Longo BM, Mello LE (1997) Blockade of pilocarpine- or kainate-induced mossy fiber sprouting by cycloheximide does not prevent subsequent epileptogenesis in rats. Neurosci Lett 226:163-166.

Longo BM, Mello LE (1998) Supragranular mossy fiber sprouting is not necessary for spontaneous seizures in the intrahippocampal kainate model of epilepsy in the rat. Epilepsy Res 32:172-182.

Lovinger DM, Colley PA, Akers RF, Nelson RB, Routtenberg A (1986) Direct relation of long-term synaptic potentiation to phosphorylation of membrane protein F1, a substrate for membrane protein kinase C. Brain Res 399(2):205-211.

Lurton D, Cavalheiro EA (1997) Neuropeptide-Y immunoreactivity in the pilocarpine model of temporal lobe epilepsy. Exp Brain Res 116:186-190.

Magloczky Z, Wittner L, Borhegyi Z, Halasz P, Vajda J, Czirjak S, Freund TF (2000) Changes in the distribution and connectivity of interneurons in the epileptic human dentate gyrus. Neuroscience 96:7-25.

Margerison JH, Corsellis JA (1966) Epilepsy and the temporal lobes. A clinical, electroencephalographic and neuropathological study of the brain in epilepsy, with particular reference to the temporal lobes. Brain 89:499-530.

Marksteiner J, Ortler M, Bellmann R, Sperk G (1990) Neuropeptide Y biosynthesis is markedly induced in mossy fibers during temporal lobe epilepsy of the rat. Neurosci Lett 112:143-148.

Mathern GW, Bertram EH, 3rd, Babb TL, Pretorius JK, Kuhlman PA, Spradlin S, Mendoza D (1997) In contrast to kindled seizures, the frequency of spontaneous epilepsy in the limbic status model correlates with greater aberrant fascia dentata excitatory and inhibitory axon sprouting, and increased staining for N-methyl-D-aspartate, AMPA and GABA(A) receptors. Neuroscience 77:1003-1019.

McCarthy JB, Walker M, Pierce J, Camp P, White JD (1998) Biosynthesis and metabolism of native and oxidized neuropeptide Y in the hippocampal mossy fiber system. J Neurochem 70:1950-1963.

McNamara RK, Routtenberg A (1995) NMDA receptor blockade prevents kainate induction of protein F1/GAP-43 mRNA in hippocampal granule cells and subsequent mossy fibre sprouting in the rat. Brain Res Mol Brain Res 33:22–8.

Meberg PJ, Gall CM, Routtenberg A (1993) Induction of F1/GAP-43 gene expression in hippocampal granule cells after seizures [corrected]. Brain Res Mol Brain Res 17(3-4):295-299.

Meldrum BS (2002) Concept of activity-induced cell death in epilepsy: historical and contemporary perspectives. Prog Brain Res. 135:3-11.

Mello LE, Cavalheiro EA, Tan AM, Kupfer WR, Pretorius JK, Babb TL, Finch DM (1993) Circuit mechanisms of seizures in the pilocarpine model of chronic epilepsy: cell loss and mossy fiber sprouting. Epilepsia 34:985-995.

Mello LE, Covolan L (1996) Spontaneous seizures preferentially injure interneurons in the pilocarpine model of chronic spontaneous seizures. Epilepsy Res. Dec; 26(1):123-9

Melloni RH Jr, Hemmendinger LM, Hamos JE, DeGennaro LJ (1993) Synapsin I gene expression in the adult rat brain with comparative analysis of mRNA and protein in the hippocampus. J Comp Neurol 327:507-520.

Mulle C, Sailer A, Perez-Otano I, Dickinson-Anson H, Castillo PE, Bureau I (1998) Altered synaptic physiology and reduced susceptibility to kainate-induced seizures in GluR6-deficient mice. Nature, 392(6676), 601-605.

Mundigl O, Matteoli M, Daniell L (1993) Synaptic vesicle proteins and early endosomes in cultured hippocampal neurones: differential effects of Brefeldin A in axon and dendrites. J Cell Biol 122:1207–21.

Nadler JV, Perry BW, Cotman CW (1980) Selective reinnervation of hippocampal area CA1 and the fascia dentata after destruction of CA3-CA4 afferents with kainic acid. Brain Res 182:1-9.

Nadler JV, Tu B, Timofeeva O, Jiao Y, Herzog H (2007) Neuropeptide Y in the recurrent mossy fiber pathway. Peptides 28:357-364.

Naffah-Mazzacoratti MG, Funke MG, Sanabria ER, Cavalheiro EA (1999) Growth-associated phosphoprotein expression is increased in the supragranular regions of the dentate gyrus following pilocarpine-induced seizures in rats. Neuroscience 91:485–92.

Nitsch R, Leranth C (1993) Calretinin immunoreactivity in the monkey hippocampal formation--II. Intrinsic GABAergic and hypothalamic non-GABAergic systems: an experimental tracing and co-existence study. Neuroscience 55:797-812.

Okazaki MM, Molnar P, Nadler JV (1999) Recurrent mossy fiber pathway in rat dentate gyrus: synaptic currents evoked in presence and absence of seizure-induced growth. J Neurophysiol 81(4):1645-1660.

Paoletti P, Neyton J (2007) NMDA receptor subunits: function and pharmacology. Curr Opin Pharmacol, 7(1), 39-47.

Paoletti P, Vergnano AM, Barbour B, Casado M (2009) Zinc at glutamatergic synapses. Neuroscience 158:126-136.

Park HG, Yu HS, Park S, Ahn YM, Kim YS, Kim SH (2014) Repeated treatment with electroconvulsive seizures induces HDAC2 expression and down-regulation of NMDA receptor-related genes through histone deacetylation in the rat frontal cortex. Int J Neuropsychopharmacol, 17(9), 1487-1500.

Patel A, Bulloch K (2003) Type II glucocorticoid receptor immunoreactivity in the mossy cells of the rat and the mouse hippocampus. Hippocampus 13:59-66.

Paternain AV, Herrera MT, Nieto MA, Lerma J (2000) GluR5 and GluR6 kainate receptor subunits coexist in hippocampal neurons and coassemble to form functional receptors. J Neurosci, 20(1), 196-205.

Pei Y, Zhao D, Huang J, Cao L (1983) Zinc-induced seizures: a new experimental model of epilepsy. Epilepsia 24:169-176.

Pierce JP, Melton J, Punsoni M, McCloskey DP, Scharfman HE (2005) Mossy fibers are the primary source of afferent input to ectopic granule cells that are born after pilocarpine-induced seizures. Exp Neurol, 196(2), 316-331

Portelli J, Aourz N, De Bundel D, Meurs A, Smolders I, Michotte Y (2009) Intrastrain differences in seizure susceptibility, pharmacological response and basal neurochemistry of Wistar rats. Epilepsy Res, 87(2-3), 234-246.

Proper EA, Oestreicher AB, Jansen GH (2000) et al. Immunohistochemical characterization of mossy fibre sprouting in the hippocampus of patients with pharmaco-resistant temporal lobe epilepsy. Brain 123 (Pt 1):19–30.

Ramon y Cajal S. (1911). Histologie du Systeme Nerveux de l'Homme et des Vertebretes. Paris: Malione

Ribak CE, Seress L, Amaral DG (1985) The development, ultrastructure and synaptic connections of the mossy cells of the dentate gyrus. J Neurocytol 14:835-857.

Riban V, Bouilleret V, Pham-Le BT, Fritschy JM, Marescaux C, Depaulis A (2002) Evolution of hippocampal epileptic activity during the development of hippocampal sclerosis in a mouse model of temporal lobe epilepsy. Neuroscience 112 (1), 101–111.

Rizzi M, Monno A, Samanin R, Sperk G, Vezzani A (1993) Electrical kindling of the hippocampus is associated with functional activation of neuropeptide Y-containing neurons. Eur J Neurosci 5:1534-1538.

Rodriguez-Moreno A, Sihra TS (2007) Metabotropic actions of kainate receptors in the CNS. J Neurochem, 103(6), 2121-2135.

Rosahl TW, Spillane D, Missler M, Herz J, Selig DK, Wolff JR, Hammer RE, Malenka RC, Sudhof TC (1995) Essential functions of synapsins I and II in synaptic vesicle regulation. Nature 375:488-493.

Ruiz AJ, Kullmann DM (2012) Ionotropic receptors at hippocampal mossy fibers: roles in axonal excitability, synaptic transmission, and plasticity. Front Neural Circuits, 6, 112.

Scharfman HE (1995) Electrophysiological evidence that dentate hilar mossy cells are excitatory and innervate both granule cells and interneurons. J Neurophysiol 74:179-194.

Scharfman HE, Gray WP (2006) Plasticity of neuropeptide Y in the dentate gyrus after seizures, and its relevance to seizure-induced neurogenesis. EXS 193-211.

Scharfman HE, Smith KL, Goodman JH, Sollas AL (2001) Survival of dentate hilar mossy cells after pilocarpine-induced seizures and their synchronized burst discharges with area CA3 pyramidal cells. Neuroscience 104:741-759.

Scharfman HE, Sollas AL, Smith KL, Jackson MB, Goodman JH (2002) Structural and functional asymmetry in the normal and epileptic rat dentate gyrus. J Comp Neurol 454:424-439.

Schauwecker PE and Steward O (1997) Genetic determinants of susceptibility to excitotoxic cell death: implications for gene targeting approaches. Proc Natl Acad Sci U S A, 94(8), 4103-4108.

Schauwecker PE (2003) Differences in ionotropic glutamate receptor subunit expression are not responsible for strain-dependent susceptibility to excitotoxininduced injury. Brain Res. Mol. Brain Res. 112 (1–2), 70–81.

Schauwecker PE (2012) Strain differences in seizure-induced cell death following pilocarpine-induced status epilepticus. Neurobiol Dis, 45(1), 297-304.

Scimemi A, Schorge S, Kullmann DM, Walker MC (2005) Epileptogenesis is Associated with Enhanced Glutamatergic Transmission in the Perforant Path. Journal of Neurophysiology. 95 (2): 1213–20.

Seress L, Abraham H, Horvath Z, Doczi T, Janszky J, Klemm J, Byrne R, Bakay RA (2009) Survival of mossy cells of the hippocampal dentate gyrus in humans with mesial temporal lobe epilepsy. J Neurosurg 111(6):1237-1247.

Sihra TS, Flores G, Rodriguez-Moreno A (2014) Kainate receptors: multiple roles in neuronal plasticity. Neuroscientist, 20(1), 29-43.

Silva JG, Mello LE (2000) The role of mossy cell death and activation of protein synthesis in the sprouting of dentate mossy fibers: evidence from calretinin and neo-timm staining in pilocarpine-epileptic mice. Epilepsia 41 Suppl 6:S18-23.

Skene JH, Jacobson RD, Snipes GJ, McGuire CB, Norden JJ, Freeman JA (1986) A protein induced during nerve growth (GAP-43) is a major component of growth-cone membranes. Science 233:783–6.

Sloviter RS (1987) Decreased hippocampal inhibition and a selective loss of interneurons in experimental epilepsy. Science 235:73-76.

Sloviter RS (1991) Permanently altered hippocampal structure, excitability, and inhibition after experimental status epilepticus in the rat: the "dormant basket cell" hypothesis and its possible relevance to temporal lobe epilepsy. Hippocampus 1:41-66.

Soriano E, Frotscher M (1994) Mossy cells of the rat fascia dentata are glutamate-immunoreactive. Hippocampus 4:65-69.

Soriano F X, Papadia S, Hofmann F, Hardingham N R, Bading H, Hardingham G E (2006) Preconditioning doses of NMDA promote neuroprotection by enhancing neuronal excitability. J Neurosci, 26(17), 4509-4518.

Sperk G, Marksteiner J, Gruber B, Bellmann R, Mahata M, Ortler M (1992) Functional changes in neuropeptide Y- and somatostatin-containing neurons induced by limbic seizures in the rat. Neuroscience 50:831-846.

Swanson LW, Wyss JM, Cowan WM (1978) An autoradiographic study of the organization of intrahippocampal association pathways in the rat. J Comp Neurol 181:681-715.

Takacs VT, Freund TF, Gulyas AI (2008) Types and synaptic connections of hippocampal inhibitory neurons reciprocally connected with the medial septum. Eur J Neurosci 28:148-164.

Tang FR, Chia SC, Zhang S, Chen PM, Gao H, Liu CP, Khanna S, Lee WL (2005) Glutamate receptor 1-immunopositive neurons in the gliotic CA1 area of the mouse hippocampus after pilocarpine-induced status epilepticus. Eur J Neurosci 21(9):2361-2374.

Telfeian AE, Federoff HJ, Leone P, During MJ, Williamson A (2000) Overexpression of GluR6 in rat hippocampus produces seizures and spontaneous nonsynaptic bursting in vitro. Neurobiol Dis, 7(4), 362-374.

Tolner EA, van Vliet EA, Holtmaat AJ, Aronica E, Witter MP, da Silva FH, Gorter JA (2003) GAP-43 mRNA and protein expression in the hippocampal and parahippocampal region during the course of epileptogenesis in rats. Eur J Neurosci 17:2369–80.

Toth K, Borhegyi Z, Freund TF (1993) Postsynaptic targets of GABAergic hippocampal neurons in the medial septum-diagonal band of broca complex. J Neurosci 13:3712-3724.

Turski WA, Cavalheiro EA, Bortolotto ZA, Mello LM, Schwarz M, Turski L (1984) Seizures produced by pilocarpine in mice: a behavioral, electroencephalographic and morphological analysis. Brain Res 321:237-253.

Turski WA, Czuczwar SJ, Kleinrok Z, Turski L (1983) Cholinomimetics produce seizures and brain damage in rats. Experientia 39:1408-1411.

Vezzani A, Michalkiewicz M, Michalkiewicz T, Moneta D, Ravizza T, Richichi C, Aliprandi M, Mule F, Pirona L, Gobbi M, Schwarzer C, Sperk G (2002) Seizure susceptibility and epileptogenesis are decreased in transgenic rats overexpressing neuropeptide Y. Neuroscience 110:237-243.

Vezzani A, Sperk G (2004) Overexpression of NPY and Y2 receptors in epileptic brain tissue: an endogenous neuroprotective mechanism in temporal lobe epilepsy? Neuropeptides 38:245-252.

Vincent P, Mulle C (2009) Kainate receptors in epilepsy and excitotoxicity. Neuroscience, 158(1), 309-323.

Volz F, Bock HH, Gierthmuehlen M, Zentner J, Haas CA, Freiman TM (2011) Stereologic estimation of hippocampal GluR2/3- and calretinin-immunoreactive hilar neurons (presumptive mossy cells) in two mouse models of temporal lobe epilepsy. Epilepsia 52:1579-1589.

Wasterlain CG, Fujikawa DG, Penix L, Sankar R (1993) Pathophysiological mechanisms of brain damage from status epilepticus. Epilepsia 34 Suppl 1:S37-53.

Wenthold RJ, Trumpy VA, Zhu WS, Petralia RS (1994) Biochemical and assembly properties of GluR6 and KA2, two members of the kainate receptor family, determined with subunit-specific antibodies. J Biol Chem, 269(2), 1332-1339.

Williamson A, Spencer D (1995) Zinc reduces dentate granule cell hyperexcitability in epileptic humans. Neuroreport 6:1562-1564.

Winawer MR, Makarenko N, McCloskey DP, Hintz TM, Nair N, Palmer AA, Scharfman HE (2007) Acute and chronic responses to the convulsant pilocarpine in DBA/2J and A/J mice. Neuroscience 149:465-475.

Zhang W, Yamawaki R, Wen X, Uhl J, Diaz J, Prince DA, Buckmaster PS (2009) Surviving hilar somatostatin interneurons enlarge, sprout axons, and form new synapses with granule cells in a mouse model of temporal lobe epilepsy. J Neurosci 29:14247-14256.

Zimmer J (1971) Ipsilateral afferents to the commissural zone of the fascia dentata, demonstrated in decommissurated rats by silver impregnation. J Comp Neurol 142:393-416.

Zimmer J (1973) Changes in the Timm sulfide silver staining pattern of the rat hippocampus and fascia dentata following early postnatal deafferentation. Brain Res 64:313-326.